Secretory production in Escherichia coli of a GH46 chitosanase from Chromobacterium violaceum, suitable to generate antifungal chitooligosaccharides

Mayara I.G. Azevedo, Simone T. Oliveira, Christiana F.B. Silva, Rômulo F. Carneiro, Celso S. Nagano, Ana C.S. Gadelha, Davi C. Torres, José E. Monteiro-Júnior, Matheus S. Girão, Celli R. Muniz, Cleverson D.T. Freitas, Thalles B. Grangeiro

PII: S0141-8130(20)34583-9

DOI: https://doi.org/10.1016/j.ijbiomac.2020.09.221

Reference: BIOMAC 16851

To appear in: *International Journal of Biological Macromolecules*

Received date: 16 June 2020

Revised date: 18 September 2020

Accepted date: 24 September 2020

Please cite this article as: M.I.G. Azevedo, S.T. Oliveira, C.F.B. Silva, et al., Secretory production in Escherichia coli of a GH46 chitosanase from Chromobacterium violaceum, suitable to generate antifungal chitooligosaccharides, *International Journal of Biological Macromolecules* (2018), https://doi.org/10.1016/j.ijbiomac.2020.09.221

Secretory production in *Escherichia coli* of a GH46 chitosanase from *Chromobacterium violaceum*, suitable to generate antifungal chitooligosaccharides

Mayara I. G. Azevedo[a], Simone T. Oliveira[a], Christiana F. B. Silva[b], Rômulo F. Carneiro[c], Celso S. Nagano[c], Ana C. S. Gadelha[d], Davi C. Torres[e], José E. Monteiro-Júnior[d], Matheus S. Girão[a], Celli R. Muniz[b], Cleverson D. T. Freitas[a], Thalles B. Grangeiro[d,*]

[a] Departamento de Bioquímica e Biologia Molecular, Centro de Ciências, Universidade Federal do Ceará, Fortaleza, Ceará, Brazil

[b] Embrapa Agroindústria Tropical, Fortaleza, Ceará, Brazil

[c] Departamento de Engenharia de Pesca, Centro de Ciências Agrárias, Universidade Federal do Ceará, Fortaleza, Ceará, Brazil

[d] Laboratório de Genética Molecular, Departamento de Biologia, Centro de Ciências, Universidade Federal do Ceará, Fortaleza, Ceará, Brazil

[e] Hospital Israelita Albert Einstein, São Paulo, SP, Brazil

* To whom all correspondence should be addressed

Prof. Dr. Thalles Barbosa Grangeiro

Laboratório de Genética Molecular, Departamento de Biologia, Centro de Ciências, Universidade Federal do Ceará, Campus do Pici, Fortaleza-CE, 60.440-900, Brazil

E-mail: thalles@ufc.br

Abstract

A chitosanase (*Cv*Csn46) from *Chromobacterium violaceum* ATCC 12472 was produced in *Escherichia coli*, purified, and partially characterized. When subjected to denaturing polyacrylamide gel electrophoresis, the enzyme migrated as two protein bands (38 and 36 kDa apparent molecular masses), which were both identified as *Cv*Csn46 by mass spectrometry. The enzyme hydrolyzed colloidal chitosan, with optimum catalytic activity at 50 °C, and two optimum pH values (at pH 6.0 and pH 11.0). The chitosanolytic activity of *Cv*Csn46 was enhanced by some ions (Ca^{2+}, Co^{2+}, Cu^{2+}, Sr^{2+}, Mn^{2+}) and DTT, whereas Fe^{2+}, SDS and β-mercaptoethanol completely inhibited its activity. *Cv*Csn46 showed a non-Michaelis-Menten kinetics, characterized by a sigmoidal velocity curve (R^2 = 0.9927) and a Hill coefficient of 3.95. ESI-MS analysis revealed that the hydrolytic action of *Cv*Csn46 on colloidal chitosan generated a mixture of low molecular mass chitooligosaccharides, containing from 2 to 7 hexose residues, as well as D-glucosamine. The chitosan oligomers generated by *Cv*Csn46 inhibited *in vitro* the mycelial growth of *Lasiodiplodia theobromae*, significantly reducing mycelium extension and inducing hyphal morphological alterations, as observed by scanning electron microscopy. *Cv*Csn46 was characterized as a versatile biocatalyst that produces well-defined chitooligosaccharides, which have potential to control fungi that cause important crop diseases.

Keywords

Chitosanase; *Chromobacterium violaceum*; chitooligosaccharides

1. Introduction

Chitin [(1→4)-2-acetamido-2-deoxy-β-D-glucan] is a natural polysaccharide widely found in terrestrial and aquatic ecosystems, consisting of linear chains of β-(1→4)-linked residues of *N*-acetyl-β-D-glucosamine (2-acetamido-2-deoxy-β-D-glucopyranose; GlcNAc) [1]. Chitin plays a structural role in many groups of organisms, being for example an important component of the cell wall of most fungi and a major constituent of the exoskeleton of arthropods [2] and [3]. The worldwide production rate of chitin has been estimated as being approximately 10^{10}-10^{11} tons per year, which makes this polysaccharide one the most abundant renewable biopolymers in nature [4].

Due to its high degree of acetylation (DA), which is usually >90%, chitin is insoluble in most ordinary solvents such as water, organic solvents, and mild acidic and basic solutions. This physicochemical property is a major factor that has limited the development of practical applications of chitin, despite its abundance, low cost, biodegradability and non-toxicity to humans [5]. Chitosan, the main *N*-deacetylated derivative of chitin, is composed of randomly distributed units of *N*-acetyl-β-D-glucosamine and β-D-glucosamine (2-amino-2-desoxi-β-D-glucopyranose; GlcN). The cell walls of some Zygomycota fungi characteristically contain, alongside chitin and β-glucans, significant contents of chitosan, which is produced *in vivo* by secreted chitin deacetylases acting on nascent chitin chains [6].

Chitosan has a degree of deacetylation (DDA) greater than 60%, being usually obtained for commercial purposes from chitin of crustaceans, which are subjected to chemical or enzymatic deacetylation reactions. At acidic pH values (pH < 6.3), the NH_2 groups on the C-2 atoms of the GlcN residues of chitosan are protonated, and the polysaccharide is converted to a water-soluble cationic polyelectrolyte [7]. The unique and versatile physicochemical properties of chitosan have stimulated numerous researches, and a wide range of potential applications have been proposed for this biopolymer in different areas, such as biomedicine,

agriculture as well as food and pharmaceutical industries. For example, depolymerization of chitosan through chemical or enzymatic hydrolysis can be used to generate low molecular mass chitooligosaccharides (COS), which have attracted the attention of biotechnologists due to the biological effects these molecules can elicit, including anticancer, antimicrobial, antiviral and antioxidant activities [8].

Chitosanases (EC 3.2.1.132; chitosan *N*-acetylglucosaminohydrolase) are glycoside hydrolases (GHs) that catalyze the endo-hydrolysis of β-(1→4)-glycosidic linkages that connect the hexose residues in chitosan chains [9]. Based on similarities of their amino acid sequences and three-dimensional structures, chitosanases are classified in 7 GH families (GH3, GH5, GH7, GH8, GH46, GH75 and GH80), according to the classification system of the carbohydrate-active enzymes database (CAZy) [10]. Three of these families (GH46, GH75 and GH80) contain only chitosanases, whereas the other 4 families (GH3, GH5, GH7 and GH8) contain chitosanases as well as enzymes with other substrate specificities, such as cellulases and xylanases [11]. Chitosanases occur in viruses, bacteria, cyanobacteria, fungi and plants, all of them sharing the ability to cleave GlcN-GlcN bonds in partially acetylated chitosan. Based on further characterization regarding substrate specificity, chitosanases have been grouped into four classes (I-IV). Therefore, class I chitosanases can additionally cleave GlcNAc-GlcN bonds, whereas class III members can also cleave GlcN-GlcNAc links. The hydrolytic activity of class II chitosanases is restricted to GlcN-GlcN bonds, whereas class IV enzymes are able to cleave all types of bonds except GlcNAc-GlcNAc linkages [12].

Chitosanases belonging to GH46 family, which are found almost exclusively in Bacteria, have been characterized more extensively in comparison to chitosanases from other families [11]. GH46 chitosanases are inverting enzymes which adopt a typical α-helical fold, as observed in members of the lysozyme superfamily, which includes protein families GH19, GH22, GH23, GH24 and GH46 [13] and [14]. The three-dimensional structure of GH46 chitosanases is

characterized by two globular lobes that are separated by a negatively charged substrate-binding cleft. Site-directed mutagenesis and X-ray crystallography have shown that two conserved acidic residues are involved in catalysis, one Glu that acts as the general proton donor and an Asp that plays the role of the general base [15] and [16]. One major application of GH46 chitosanases is their use as precise tools for depolymerization of chitosan and production of chitosan oligomers with desired biological properties. Expression of the GH46 chitosanase Cho1 from *Bacillus circulans* MH-K1 in rice plants improved resistance to the rice blast fungus *Magnaporthe oryzae*, suggesting that bacterial chitosanases could be used to protect crops against fungal diseases [17].

Chromobacterium violaceum (β-Proteobacteria, Chromobacteriaceae) is a free-living, Gram-negative species that inhabits soil and water environments of tropical and subtropical regions [18]. Most *C. violaceum* strains form purple colonies due to the production of violacein, a secondary metabolite derived from tryptophan, which has been extensively investigated by its biological activities with potential biomedical applications, such as the ability to kill Gram-positive bacteria [19]. A secreted GH46 chitosanase has been detected in the exoproteome of *C. violaceum* ATCC 12472, but the biochemical properties of this enzyme are still unknown [20]. In the present work, aiming to verify the biotechnological potential of the *C. violaceum* GH46 chitosanase, the enzyme from the type strain ATCC 12472 (herein referred to as *Cv*Csn46) was expressed in *Escherichia coli* and secreted into the culture medium using its native signal peptide. The secreted recombinant product was then purified, its functionality was experimentally validated, and the potential of *Cv*Csn46 as well as the chitooligosaccharides generated from its hydrolytic action on chitosan, to act as antifungal agents, was evaluated.

2. Materials and methods

2.1. Bacterial cells, fungus, plasmid vectors, culture media and other reagents

Cells of *Escherichia coli* strains DH5α and BL21(DE3) and the plasmid pET303/CT-His were purchased from Invitrogen (Carlsbad, CA, USA). *Lasiodiplodia theobromae* (Pat.) Griffon & Maubl. strain CCJ-184 was isolated by Dr. C.F.B. Silva (Embrapa Agroindústria Tropical, Brazil) from infected plants of *Anacardium occidentale* L. CCP76, and preserved using the Castellani method [21]. *Chromobacterium violaceum* ATCC 12472 was a gift from Dr. T.B. Creczynski-Pasa (Federal University of Santa Catarina, Brazil). Chitosan powder (degree of deacetylation, DDA = 85%) was purchased from Polymar (Fortaleza, CE, Brazil). All other reagents were of high purity, analytical grade.

2.2. Homology modeling and molecular docking calculations

Comparative structural modeling was performed using MODELLER [22] through the MPI Bioinformatics Toolkit (https://toolkit.tuebingen.mpg.de) web service [23]. Suitable homologous sequences with known three-dimensional structures to be used as templates were selected using HHPred (https://toolkit.tuebingen.mpg.de/tools/hhpred). The chitin-binding domain (ChBD) from chitinase 60 of *Moritella marina* (PDB ID: 4MB4; percentages of sequence identity and similarity with the ChBD of *Cv*Csn46 = 28.2% and 48.7%, respectively; estimated probability of the template to be homologous to the query sequence = 96.08%) [24] and the catalytic domain (CatD) from a GH46 chitosanase of *Bacillus circulans* MH-K1 (PDB ID: 5HWA; percentages of sequence identity and similarity with the CatD of *Cv*Csn46 = 70.5% and 81.1%, respectively; estimated probability of the template to be homologous to the query sequence = 100.0%) [25] were used as template structures. The stereo-chemical quality of modeled structures (Tables S4 and S5) was evaluated using PROSESS [26]. Molecular docking calculations were performed using AutoDock Tools v. 1.5.6 [27] and AutoDock Vina v. 1.1.2 [28], as described in detail by Maranhão et al. [29].

Three-dimensional molecular models were visualized using the program PyMOL Molecular Graphics System, version 2.0 Schrödinger, LLC.

2.3. Phylogenetic analysis

Bayesian phylogenetic analysis was performed using MrBayes version 3.2.7a [30], with LG+I+G4+F as the best-fit amino acid substitution model. Best-fit substitution model was selected using the Akaike information criterion (AIC) strategy, as implemented by ModelTest-NG version 0.1.5 [31]. Two independent analyses of 10,000,000 generations were run to estimate parameters related to sequence evolution and likelihood probabilities using a Metropolis-coupled Markov Chain Monte Carlo (MCMC) method. In addition, eight simultaneous chains were initiated with random tree, sampling frequency of 500, and a diagnostic frequency of 50,000. After a 25% burn-in fraction, a 50% majority rule consensus tree was calculated including posterior probabilities (PP) as branch support estimates. Phylogenetic analysis was implemented on the CIPRES Science Gateway version 3.3 (www.phylo.org) [32]. The Bayesian majority-rule consensus tree was visualized and edited using iTOL v. 5.5 (https://itol.embl.de) [33].

2.4. Construction of the expression vectors

To express *Cv*Csn46 in *E. coli*, the full coding sequence (excluding the stop codon) of the gene *Cv3931*, corresponding to a DNA fragment with 1,080 bp, which spans the chromosome of *C. violaceum* ATCC 12472 from position 4,252,283 to 4,253,365 (GenBank accession number: AE016825), was amplified by PCR using a high-fidelity DNA polymerase and a pair of specific oligonucleotide primers (Fig. S1). This fragment encoded the native *Cv*Csn46, with a type I signal peptide at the N-terminal region (Fig.S2). The amplified fragment was cloned into the pET303/CT-His expression plasmid, using the sites for *Xba*I and *Xho*I, which

generated the vector pET303-*Cv*Csn46. This recombinant vector was used for the secretory expression of *Cv*Csn46 with a polyhistidine (6×His) tag at the C-terminal end. The expression plasmid was introduced in chemically competent cells of *E. coli* BL21(DE3), using the heat shock method, as previously described [34]. Primary transformants were selected on LB agar supplemented with 200 µg/mL carbenicillin.

2.5. Expression and purification of the recombinant product

Cells of *E. coli* BL21(DE3) harboring the recombinant plasmid pET303-*Cv*Csn46 were inoculated in LB broth, containing the appropriate antibiotic, and the culture was incubated at 37 °C under vigorous orbital shaking (180 rpm) until the optical density at 600 nm (OD_{600}) reached 0.5-0.6. Isopropyl-β-D-thiogalactopyranoside (IPTG) was then added (0.4 mM final concentration) to the culture and the cells were incubated at 37 °C, 180 rpm, for 24 h. Extracellular proteins, which were secreted into the culture medium by *E. coli* cells expressing *Cv*Csn46, were recovered by ammonium sulfate precipitation, as described by Lobo et al. [35]. Next, the recombinant product was purified by immobilized metal ion affinity chromatography (IMAC), using the resin Ni Sepharose 6 Fast Flow (GE Healthcare Bio-Sciences, Piscataway, NJ, USA).

2.6. Enzymatic assay

Chitosanase activity was determined using colloidal chitosan (10 g/L) as substrate, which was prepared according to a protocol previously described [36]. Protein samples (250 µL) were mixed with colloidal chitosan (250 µL), the mixture was incubated in a water bath for 30 min at the specified pH and temperature, and the amounts of reducing sugars were measured using the 3,5-dinitrosalicylic acid (DNS) method [37], with D-glucosamine hydrochloride as the standard. One unit (U) of chitosanase activity was defined as the amount of enzyme that

produced 1 µmol reducing sugar per minute. Visualization of chitosanase activity was performed using a plate assay, based on the procedure described by Teather and Wood [38]. Samples were loaded onto the wells of a 1% (w/v) agar plate containing 0.1% (w/v) chitosan, dissolved in 50 mM sodium acetate buffer (pH 5.2). Plates were incubated at 37 °C for 24 h, the medium was overlaid with 0.1% Congo red, incubated at room temperature for 5 min under orbital shaking, washed with distilled water and photographed.

2.7. Determination of soluble protein content

Concentration of soluble proteins was determined using the Bradford method [39]. To determine the concentration of *Cv*Csn46 in solutions containing the purified protein, the Beer-Lambert law was employed, using the protein molar extinction coefficient, calculated from its amino acid composition through the ExPASy's ProtParam tool (https://web.expasy.org/protparam/).

2.8. Electrophoresis of proteins and identification of peptides by tandem mass spectrometry

Electrophoresis of proteins under denaturing conditions (sodium dodecyl sulfate-polyacrylamide gel electrophoresis, SDS-PAGE) was performed as described by Laemmli [40], using 15% polyacrylamide slab gels. Preparation of samples prior to electrophoresis was done as described by Lobo et al. [35]. Protein bands were stained with colloidal Coomassie Brilliant Blue G-250, which was prepared as described by Candiano et al. [41]. Trypsin in-gel digestion of protein bands resolved by SDS-PAGE and identification of tryptic peptides by tandem mass spectrometry (LC-ESI-MS/MS) were performed as previously described [42].

2.9. Biochemical characterization of the purified chitosanase

The following biochemical parameters were determined for the purified recombinant enzyme, as described in detail by Lobo et al. [35]: optimal values of pH and temperature for hydrolytic activity, protein stability to distinct values of pH and temperature, and the effects of cationic ions, chelating and reducing agents and protein denaturant on enzymatic activity. The effect of different pH values on enzyme stability and catalytic activity was determined using the following buffer systems (each one in 50 mM concentration): Glycine-HCl (pH 2.0 and 3.0), acetic acid-sodium acetate (pH 4.0, 5.0 and 6.0), Tris-HCl (pH 7.0 and 8.0), Glycine-NaOH (pH 9.0, 10.0 and 11.0) and potassium chloride-NaOH (pH 12.0). All the assays were performed using 250 µg/mL *Cv*Csn46, which was incubated with 1% colloidal chitosan for 30 min, under the specified conditions, and the amounts of reducing ends were determined by the DNS method. Steady-state kinetic parameters of *Cv*Csn46 were determined using colloidal chitosan as substrate, at concentrations varying from 2.5 to 15 mg/mL. The assays were performed at pH 6.0 (protein dissolved 50 mM sodium acetate buffer) for 15 min at 50 °C, using the standard assay procedure. Plots of initial reaction velocity (V_0) *vs* substrate concentration [S], were obtained using GraphPad Prism software v.6.01. Far-UV circular dichroism (CD) spectra of *Cv*Csn46 were acquired using a Jasco J-815 spectropolarimeter (Jasco International Co., Tokyo, Japan), as previously described [43].

2.10. Production of chitooligosaccharides from chitosan

Chitosan powder was dissolved in 50 mM acetic acid to obtain a 1% (w/v) solution. Next, the purified recombinant chitosanase was added (5 µg per mL of chitosan solution) and the mixture was incubated at 50 °C for 24 h under constant agitation. To inactivate the enzyme, the mixture was heated at boiling water for 10 min, cooled at room temperature and subjected to centrifugal ultrafiltration, using a 3 kDa molecular weight cutoff concentrator (GE Healthcare). The volume of the flow-through fraction was then reduced to 1/10th of its initial

value by lyophilization and stored at 4 °C until used. Oligosaccharides concentration was determined using the DNS method.

2.11. Mass spectrometry analysis of chitooligosaccharides

Average molecular mass of chitosan oligomers was determined using ESI-MS. Samples were dissolved in 50% acetonitrile containing 0.2% (v/v) formic acid. A 100 µL (0.3 µg/µL) aliquot was centrifuged at 8,000 *g* for 5 min and loaded directly onto a nanoelectrospray ion source (nanoES) coupled to a Synapt HDMS ESI-Q-ToF mass spectrometer (Waters Corp., Milford, MA, USA). The instrument was calibrated with phosphoric acid clusters. Mass spectra were acquired by scanning at m/z range from 100 to 1,500, at a rate of 1 scan per second. The mass spectrometer was operated in positive mode, using a source temperature of 363 K and capillary voltage at 2.5 kV. Data collection and processing were controlled by Mass Lynx 4.1 software (Waters).

2.12. *In vitro* antifungal activity assay

Purified *Cv*Csn46 (3 mg/mL, dissolved in distilled water, pH 6.0) as well as chitooligosaccharides obtained from the hydrolytic action of *Cv*Csn46 on colloidal chitosan (22 mg/mL, dissolved in distilled water, pH 6.0), were evaluated regarding their ability to inhibit *in vitro* the growth of *L. theobromae* CCJ-184. Protein (dose = 300 µg) or oligosaccharides samples (doses = 2000, 1000, 500 and 250 µg) were spread on the surface of PDA (potato dextrose agar medium, pH 5.6; HiMedia Laboratories, Mumbai, India) plates (3 replicates per dose) using a Drigalski spatula and incubated at room temperature for 10 min. Next, a small disc (~ 10 mm diameter) containing fungus mycelium was placed on the center of each plate and the plates were incubated at 28 °C ± 2 °C and photoperiod of 12 h light / 12 h darkness. Mycelium diameter of each colony was measured with a pachymeter and

photographed at every 24 h. Mycelium discs inoculated on plates in which water or 5 µg Carbendazim (Derosal 500 SC, Bayer) were spread over the medium were used as controls. Samples of mycelium from colonies exposed to distilled, chitooligosaccharides (dose = 2 mg) or Carbendazim for 96 h were subjected to scanning electron microscopy (SEM). Preparation of samples and acquisition of images were performed as previously described [44].

3. Results and discussion

3.1. Structural and functional features of *Cv*Csn46, a GH46 chitosanase from *C. violaceum*

The gene *Cv3931* of *C. violaceum* ATCC 12472 encodes a protein with 360 amino acid residues, containing a 29-residues type I signal peptide (SP) at the N-terminal end, followed by a chitin-binding type 3 domain (ChtBD3; residues 50-89) and a GH46 CatD (residues 121-347) at the C-terminal region (Fig. 1A). The monoisotopic molecular mass predicted for the encoded protein was calculated as 38,431.94 Da (~ 38 kDa), with a theoretical pI = 8.99. Predicted values of molecular mass and theoretical pI for the mature protein (i.e., excluding the residues corresponding to the signal peptide) were 35,656.37 Da (~ 36 kDa) and 8.54, respectively. The ChBD of *Cv*Csn46 is closely related to the ChBD of *Streptomyces griseus* chitinase C (ChiC) (Fig. 2A). The ChBD of ChiC is a compact structure, containing β-strand segments and two Trp residues exposed on the surface, which are both necessary for binding activity to chitin, as suggested by molecular dynamics simulations and site-directed mutagenesis [45] and [46]. In the ChBD of *Cv*Csn46, the homologous aromatic residues that are likely to be involved in substrate binding are Phe^{74} and Trp^{75} (Figs. 2A and 2B). Other conserved aromatic residues in the ChBD of *Cv*Csn46 and related sequences are Trp^{51}, Tyr^{57}, Tyr^{70} and Trp^{87} (Fig. 2A). These conserved residues form a hydrophobic core that contribute to determine the compact structure of the substrate-binding domain [47]. The catalytic domain

of *Cv*Csn46 belongs to the superfamily chitosanase of CATH structural domains (CATH superfamily 3.30.386.10), whose representative structures are the chitosanases from *Bacillus circulans* MH-K1 [25] and *Streptomyces* sp. N174 [16]. In these enzymes, a Glu acts as the general acid and an Asp plays the role of the general base during catalysis. The Asp residue, with the assistance of a Thr, activates a water molecule for the nucleophilic attack on the glycosidic bond, with inversion of the stereochemistry at the anomeric carbon produced from the β(1→4)-linkage hydrolysis (Fukamizo et al., 1995). Based on the alignment of the amino acid sequence of *Cv*Csn46 with representative three-dimensional structures of bacterial chitosanases, the putative catalytic residues were identified as Glu^{138}, Asp^{156} and Thr^{161} (Fig. 3). The probable involvement of these 3 residues of *Cv*Csn46 in chitosan hydrolysis was further supported by homology modeling and molecular docking calculations (Fig. 4). When a trisaccharide [$(GlcN)_2(GlcNAc)_1$] was docked in the substrate-binding cleft of *Cv*Csn46, sugar units occupied the subsites −2 to +1 (Fig. 4B). In this protein-sugar complex model, the relative orientations, calculated distances and polar contacts of the side chains of Glu^{138}, Asp^{156} and Thr^{161} towards the bound substrate are compatible with the proposed catalytic role for these residues (Fig. 4C).

To verify the phylogenetic occurrence of proteins structurally related to *Cv*Csn46 in other strains of *C. violaceum* as well as in other species of *Chromobacterium* and related genera, BLAST searches were performed, using a local database comprising 102 proteomes from different strains and species belonging to the family Chromobacteriaceae (β-Proteobacteria; Neisseriales). This analysis revealed that, proteins sharing the same domain architecture and significant sequence identity percentage to *Cv*Csn46 (ranging from 67.9 to 100%), occur in all sampled proteomes of *C. violaceum* strains and in the proteomes of some strains of *Chromobacterium* sp., *C. haemolyticum*, *C. rhizoryzae*, *C. subtsugae*, *C. sphagni* and *C. vaccinii* (Fig. 1B). Among all other proteomes of Chromobacteriaceae, only the proteome of

Pseudogulbenkiania ferrooxidans EGD-HP2 possesses a protein related to *Cv*Csn46 (Table S3). In all these proteins, the dipeptide of the ChBD involved in substrate binding is either Phe-Trp, like found in *Cv*Csn46 (Phe^{74} and Trp^{75}), or Tyr-Trp, in which the aromatic Phe was substituted by a chemically similar Tyr residue. Furthermore, the 3 residues of the CatD, which are involved in catalysis (Glu^{138}, Asp^{156} and Thr^{161} in *Cv*Csn46), are conserved in this group of Chromobacteriaceae chitosanases (Fig. S12). Noteworthy, BLAST searches against bacterial proteomes, as available in the NCBI databases, showed that, within the order Neisseriales, which contains the families Chromobacteriaceae and Neisseriaceae, the presence of proteins related to *Cv*Csn46 is restricted to some species of *Chromobacterium* and *Pseudogulbenkiania*. Outside Neisseriales, the closest structural neighbors to *Cv*Csn46 (with sequence identity percentages ranging from 54.2 to 67.3 %) are found in species of *Collimonas* (Burkholderiales; Oxalobacteraceae), *Burkholderia*, *Paraburkholderia* and *Pandoraea* (Burkholderiales; Burkholderiaceae). Moreover, the topology of the protein tree, showing the phylogenetic relationships among *Cv*Csn46 and its structural neighbors (Fig. S13), is not congruent with the phylogenetic tree of *Chromobacterium* species, as inferred from 19 housekeeping proteins (Fig. 1B). Possibly, events of gene loss and lateral gene transfer have played a role in the evolutionary history of this group of GH46 chitosanases related to *Cv*Csn46.

To experimentally validate the hypothesis that *Cv*Csn46 is a functional chitosanase, able to convert chitosan chains into chitooligosaccharides of low molecular mass, the protein was produced in *E. coli*, purified, and partially characterized.

3.2. Purification and biochemical characterization of the recombinant chitosanase *Cv*Csn46 produced in *E. coli*

Targeting of recombinant proteins expressed in *E. coli* to the periplasmic space or culture medium has proven a suitable strategy to produce correctly folded enzymes, with simplification of downstream purification schemes [49]. Therefore, to produce *Cv*Csn46 in *E. coli*, an expression vector (pET303-*Cv*Csn46) containing a *C. violaceum* DNA fragment encoding the full sequence of *Cv*Csn46 was obtained and transformed into BL21(DE3) cells. The recombinant chitosanase *Cv*Csn46 was then purified from the cell-free culture medium of *E. coli* BL21(DE3) cells expressing pre*Cv*Csn46 using ammonium sulfate precipitation and IMAC (Fig. S3). When the purified protein was reduced and subjected to SDS-PAGE, two closely migrating protein bands with apparent molecular masses of 38 and 36 kDa were observed (Fig. 5A). These values are in agreement with the monoisotopic molecular mass calculated for the recombinant protein (36,720.85 Da), considering the cleavage of the signal peptide and the presence of 8 extra residues (LEVHHHHH) at the C-terminal end of the recombinant product, which was secreted into the culture medium by *E. coli* cells. The identity of the 38 and 36 kDa protein bands observed on SDS-PAGE as *Cv*Csn46 was confirmed by *de novo* sequencing of tryptic peptides by tandem MS analysis (Figs. S4-S9 and Table S1). Peptides identified from these bands covered ~ 64.5% (38 kDa band) and 41.3% (36 kDa band) of the primary structure of *Cv*Csn46. The behavior of *Cv*Csn46 as a doublet on SDS-PAGE can be due to partial re-oxidation of the Cys residues involved in the single intramolecular disulfide bond that was predicted to occur in the CatD (Fig. 4), producing two distinct conformational states of the same molecule, a phenomenon that has been observed in other proteins [50].

The average yield of the purified *Cv*Csn46 produced in *E. coli* was *ca*. 19 mg of recombinant protein per liter of induced culture. Far-UV CD spectra of the recombinant *Cv*Csn46 were characteristic of a folded, α-helical protein (Fig. S10), with two negative bands at 209 nm and 222 nm, separated by an indentation at 215 nm, and a positive band at 193 nm [51]. The

recombinant chitosanase was able to degrade colloidal chitosan (Fig. 5B), with a specific activity of 10,000 U/mg of protein. As a typical chitosanase, the enzyme did not show any detectable hydrolytic activity on colloidal chitin.

The hydrolytic activity of purified *Cv*Csn46 was detected over a broad pH range, with dual optimum pH values for catalysis, one at pH 6.0 and another at pH 11.0 (Fig. 6A). Moreover, *Cv*Csn46 was stable over a wide pH range (Fig. 6A), recovering a significant proportion (> 85%) of its full catalytic activity when incubated at pH values from 2 to 12 and next subjected to enzymatic assay at its optimum acidic pH (pH 6.0). Comparable to this amphiprotic behavior of *Cv*Csn46, a GH8 chitosanase from *B. mycoides* exhibited optimum activity at pH values 6.0 and 10.0 [52]. Significant hydrolytic activity of *Cv*Csn46 (> 90% relative activity), measured at pH 6.0, was observed when the enzymatic assay was performed at temperatures from 40 °C to 60 °C, the highest catalytic activity being recorded at 50 °C (Fig. 6B). However, the recombinant enzyme exhibited negligible or no detectable hydrolytic activity when incubated for 1 h at temperatures equal or above 50 °C and then subjected to enzymatic assay at pH 6.0 (Fig. 6B). The midpoint temperature of the unfolding transition (T_m) was determined as 54.6 °C (Fig. S1D). Therefore, binding of polymeric chitosan to *Cv*Csn46 leads to enhanced thermal stability of the recombinant product, and a similar effect of substrate binding on the conformational stability of a protein has been reported for other enzymes [53]. Some metal ions (Pb^{2+}, Fe^{3+}, La^{2+}, Hg^{2+}, Ni^{2+}, Ag^{+} and Rb^{+}) significantly ($P < 0.05$) reduced *Cv*Csn46 activity, with Fe^{3+} completely abolishing the enzyme ability to degrade colloidal chitosan (Fig. 6C). Metal ions bind to residues at the catalytic sites of many glycoside hydrolases, effectively inhibiting their enzymatic activity. It has been speculated that the interaction of metal ions with side chain carboxylate groups of critical catalytic residues fix their conformation, thus restricting their hydrolytic capabilities [54]. In the case of *Cv*Csn46, treatment with 5 mM Fe^{3+} caused a drastic alteration in the protein conformation,

as revealed by CD spectroscopy (Fig. S10B). Conversely, another group of cationic ions (Ca^{2+}, Co^{2+}, Cu^{2+}, Sr^{2+} and Mn^{2+}) significantly ($P < 0.05$) increased the hydrolytic activity of *Cv*Csn46, notably Cu^{2+} (*ca*. 2.6-fold increase) and Mn^{2+} (approximately 3.8-fold increment). All tested concentrations of SDS (0.5, 1.0 and 2.0%) and treatment with 5 mM β-mercaptoethanol completely abolished the enzymatic activity of *Cv*Csn46 (Fig. 6D). When treated with ethylenediaminetetraacetic acid (EDTA), *Cv*Csn46 activity was either diminished (83-90% relative activity) or had a slight increase (108% relative activity). Contrary to the inhibiting effect of β-mercaptoethanol, the enzymatic activity of *Cv*Csn46 significantly increased ($P < 0.05$) when exposed to dithiothreitol (DTT) at concentrations of 50 mM (123% relative activity) and 100 mM (170% relative activity). The stimulatory effect of DTT on the catalytic activity of other enzymes has been reported, but the mechanism involved is still poorly understood [55] and [56]. Altogether, these results suggest that, probably, *Cv*Csn46 is not a metalloenzyme, but relies on the presence of cation ions (Mn^{2+}, for example) and the reducing agent DTT, to express its maximal catalytic activity. Furthermore, the single disulfide bond in the CatD of *Cv*Csn46 was predicted to link the side chains thiol groups of Cys^{151} and Cys^{225} (Figs. 3 and S9), likely plays an essential role in maintaining the protein properly folded and hence enzymatically active. This assumption is supported by the inhibitory effect of β-mercaptoethanol, which probably inhibits *Cv*Csn46 activity by reducing this disulfide bridge. Therefore, the enhancement of *Cv*Csn46 activity caused by DTT is unlikely to be related to thiol-disulfide exchange reaction, supporting previous observations that DTT can affect protein function by a mechanism distinct from its ability to protect thiol groups [57].

Plots of initial velocity of chitosan degradation catalyzed by *Cv*Csn46 fitted a sigmoid curve ($R^2 = 0.9927$), revealing a non-Michaelis-Menten kinetics (Fig. 5C). Kinetics parameters were V_{max} = 10,818.0 μmol/min/mg, K_m = 3.06 mg/mL, k_{cat} (turnover number) = 4,008.19 min^{-1},

and k_{cat}/K_m (catalytic efficiency) = 1,309.86 mL mg^{-1} min^{-1}. The Hill coefficient was 3.95, indicating positively cooperative binding between *Cv*Csn46 and the substrate chitosan, which is probably linked to protein conformational changes induced by the substrate. A chitosanase from *Bacillus* sp. MN has also shown a sigmoidal kinetics, with a positive Hill coefficient of 1.54, determined in enzymatic assays using polymeric chitosan with DA = 10% [58]. GH46 chitosanases exhibit an α-helical fold, characterized by two globular lobes separated by the substrate-binding groove [16] and [25], as depicted in Fig. 4. Moreover, Lyu et al. have demonstrated that, in chitosanase OU01 from *Pseudomonas* sp. A-01, notable conformational changes are induced by substrate binding to the catalytic cleft, including a rotation of lobes A and B relative to each other [59]. Therefore, considering the close structural relationship between *Cv*Csn46 and OU01 (RMSD = 1.361 Å; Fig. S13), binding of polymeric chitosan to *Cv*Csn46 could also induce similar conformational changes.

When the low molecular mass products released from colloidal chitosan incubated with *Cv*Csn46 were analyzed by ESI-MS, an array of positive ion clusters with a degree of polymerization (DP) ranging from 1 to 6 was observed (Fig. 7 and Fig. S11). These ion clusters corresponded to GlcN, $(GlcN)_2$, $(GlcN)_3$, $(GlcN)_1(GlcNAc)_2$, $(GlcN)_2(GlcNAc)_1$, $(GlcN)_4$, $(GlcN)_5$, and $(GlcN)_6$. A time course analysis revealed that this ion clusters profile remained almost unchanged from 4 h to 24 h of digestion, except for the presence of an ion cluster corresponding to the heptasaccharide $(GlcN)_7$, which was transiently found at time point 16 h (Fig. S11 and Table S2). The pattern of chitosan degradation by *Cv*Csn46, showing a continuum of oligomeric products with DP values ranging from 2 to 6, is diagnostic of a non-processive endo-acting enzyme. On the other hand, the concomitant release of GlcN from polymeric chitosan indicates that *Cv*Csn46 also behaves as an exo-acting enzyme, with β-exo-glucosaminidase activity. Moreover, the presence of chitosan oligomers with DP = 2-6 over a 24 h time reaction shows that the endo-type activity of *Cv*Csn46 outweighs its exo-mode

cleavage activity. This mode of hydrolytic action of *Cv*Csn46 is distinct from that exhibited by most chitosanolytic enzymes characterized to date, which hydrolyze polymeric chitosan and chitosan oligomers using exclusively an endo-type catalytic mode [11]. Conversely, a few chitosanases degrade chitosan chains employing an exo-type cleavage pattern [60]. Similarly to the dual cleavage pattern of *Cv*Csn46, Zhang et al. have described the characterization of a GH18 chitinase from *Chitinolyticbacter meiyuanensis* SYBC-H1 (*Cm*Chi1) that behaves differently in comparison to typical chitinases, displaying both endo- and exo-type activities towards *N*-acetyl chitooligosaccharides and colloidal chitin. But different from *Cv*Csn46, the exo-type activity of *Cm*Chi1 outweighs its endo-type cleavage pattern [61].

3.3. Antifungal activity of chitooligosaccharides produced by the hydrolytic action of *Cv*Csn46 on chitosan

Chitosan is characteristically present as a structural component in the cell wall of some Zygomycota fungi, such as those of the genera *Absidia*, *Mucor*, and *Rhizopus* [62]. However, there are some non-Zygomycota species that also contain substantial amounts of chitosan in their cell walls, such as *Fusarium oxysporum*, a filamentous Ascomycota species with many plant pathogenic strains [63]. Consequently, the mycelial growth of these chitosan-containing fungi is usually suppressed *in vitro* by chitosanases [64].

Lasiodiplodia theobromae is a phytopathogenic, filamentous Ascomycota of the family Botryosphaeriaceae. It can infect a wide range of host plants in tropical and subtropical regions, causing different diseases, such as dieback, root rot, blights and gummosis, with significant economic losses in many countries [65]. On rare occasions, this cosmopolitan species can also infect humans, causing subcutaneous phaeohyphomycosis [66] and keratitis [67]. To evaluate whether *Cv*Csn46 could reduce or suppress the growth of this phytopathogenic fungi, a colony of *L. theobromae* CCJ-184 was exposed *in vitro* to a dose of

300 µg of the purified enzyme. Under these experimental conditions, no suppression or reduction in mycelial growth was observed. Contrarily, *L. theobromae* mycelium exposed to the recombinant protein grew up faster when compared to colonies of control plates (Fig. S17). However, a mixture of chitosan fragments derived from the hydrolytic action of *Cv*Csn46 on polymeric chitosan, as characterized by ESI-MS analysis (Fig. 7), strongly inhibited the growth of *L. theobromae* CCJ-184 colonies (Fig. S17). The inhibitory effect lasted until 96 h after the beginning of the bioassay, when the inhibition indexes varied from ~ 59.4% (dose = 0.25 mg) to 83.8% (dose = 2 mg). Indeed, mean diameters of fungus colonies grown in the presence of different doses of chitooligosaccharides were significantly ($P < 0.0001$) lower in comparison to the mean diameter of control colonies, measured at time points of 48 h, 72 h and 96 h (Fig. 8). These data showed that *L. theobromae* CCJ-184 is sensitive to low molecular mass chitooligosaccharides. To verify possible morphological alterations in fungal mycelium exposed to COS produced from chitosan by the hydrolytic action of *Cv*Csn46, samples of treated mycelium were observed by SEM (Fig. 8). Hyphae of untreated mycelium had a normal appearance, characterized by a dense network of long, interwoven, tubular structures, displaying a smooth, uniform surface (Figs. 8A-C). On the other hand, mycelia that were exposed to COS exhibited a disorganized array of much shorter and thinner hyphae, showing several morphological alterations (Figs. 8D-G). Some of these morphological alterations induced by COS included hyphae with a moniliform appearance, characterized by adjacent swollen segments, as shown in Fig. 8G. Furthermore, alterations in hyphal tips were also observed. Some hyphal tips appeared swollen, forming sometimes large bulges, whereas in other hyphae, the tips were completely absent (Fig. 8G). When the COS mixture generated by *Cv*Csn46 was tested on two isolates of the *Fusarium fujikuroi* species complex (FFSC), no *in vitro* inhibition of colony growth was observed (Fig. S18), indicating that these isolates are resistant to chitosan oligomers. Differences in the composition of the

plasma membrane and cell wall among fungi species have been suggested as key determinants for their sensitivity or resistance to chitosan [68] and [69]. Therefore, COS released from colloidal chitosan treated with *Cv*Csn46 was able to effectively inhibit the growth of an isolate of the phytopathogenic fungus *L. theobromae*, inducing morphological alterations in hyphae and hyphal tips, as revealed by SEM analysis.

GH46 chitosanases from *B. circulans* MH-K1 and *Amycolatopsis* sp. CsO-2 have been shown to inhibit the growth of Zygomycota species that contain chitosan as a cell wall component, and in both cases, the ability of each enzyme to cleave chitosan was essential for their antifungal activities [70] and [71]. Details on the biochemical composition and structural organization of the cell wall of *L. theobromae* have not been described. Therefore, we can hypothesize that the absence of mycelial growth inhibition of *L. theobromae*, when exposed *in vitro* to *Cv*Csn46, is likely due to the chemical composition of the cell wall of this phytopathogen, which probably has relatively low amounts of chitosan.

Despite the lack of antifungal activity against *L. theobromae*, *Cv*Csn46 generated a mixture of chitosan chitooligosaccharides with a well-defined DP range (DP = 2-6), that significantly inhibited *in vitro* the mycelium growth of this important phytopathogen, causing notable morphological alterations, as revealed by SEM images. Previously, Yuan et al. [72] showed that polymeric chitosan (DDA = 95% and average molecular weight = 230 kDa) caused *in vitro* growth inhibition of 3 *Lasiodiplodia* species (*L. rubropurpurea*, *L. crassispora*, and *L. theobromae*). At the highest concentration tested (400 mg/L), inhibitory indexes were, approximately, 34.6% (*L. crassispora*), 36.9% (*L. theobromae*) and 37.8% (*L. rubropurpurea*). Higher inhibitory indexes (70.2-76.7%) were achieved when a surfactin-β-cyclodextrin-chitosan conjugate was tested (at 400 mg/L) against the 3 *Lasiodiplodia* species.

The results of the present work show that a mixture of water-soluble, low molecular mass chitosan oligomers, which can be produced using a simple and low-cost protocol, is as effective as a complex chitosan nanosystem in inhibiting the growth of *L. theobromae*.

In the *in vitro* bioassays that evaluated the antifungal potential of the chitosan oligomers generated by *Cv*Csn46, the oligomers were dissolved in water with an acidic pH (pH = 6.0), and the oligomers sample as well as the mycelial inoculum were placed on PDA agar medium with pH = 5.6. Moreover, it is known that the amino groups on the C-2 atoms of the GlcN residues in chitosan chains have a p$K_a \approx 6.3$ [7]. Therefore, under these experimental conditions, the chitosan oligomers are positively charged, due to the cations (NH_3^+) attached to the C-2 atoms of individual GlcN residues. This chemical feature suggests a mechanism of antifungal activity that could involve binding of these positively charged chitooligosaccharides to negatively charged phospholipid molecules of fungal cell membrane, leading to disruption of cell membrane permeability and leakage of intracellular components, such as potassium ions, as indicated by a previous work on the antifungal effects of chitosan against *Ceratocystis fimbriata*, a phytopathogenic fungus that attacks sweet potato [73]. Cells of filamentous fungi grow at the hyphal tips through continuous synthesis of new cell membrane and cell wall material [74]. The morphological alterations in hyphal tips of *L. theobromae* cells, as observed in the present work, suggest that chitosan oligomers probably interfere with the synthesis of new plasma membrane, affecting hyphal apex morphology and impairing its elongation. Furthermore, chitooligosaccharides could penetrate the cell membrane and enter the cell cytoplasm and reach the nucleus, binding fungus DNA and affecting mRNA expression and protein synthesis, thus promoting fungal growth inhibition [75] and [76].

4. Conclusions

In the present work, a GH46 chitosanase from *C. violaceum* ATCC 12472 (*Cv*Csn46) was successfully expressed in *E. coli*. The native signal peptide of *Cv*Csn46 was used to direct the secretion of the recombinant product into the culture medium, a strategy that was appropriate to obtain reasonable amounts of properly folded enzyme. *Cv*Csn46 was experimentally validated as a functional chitosanolytic enzyme that can degrade polymeric chitosan, producing a mixture of low molecular mass chitooligosaccharides, with a well-defined degree of polymerization (DP = 2-6). These chitooligosaccharides were able to inhibit *in vitro* the growth of *L. theobromae*, a phytopathogen that causes important economic losses in many crops worldwide. *Cv*Csn46 exhibited some distinct biochemical features in comparison to most GH46 chitosanases currently known, such as high relative catalytic activity at both acidic and alkaline pH values, sigmoidal kinetics with positively cooperative binding, and the ability to degrade polymeric chitosan through dual endo- and exo-type hydrolytic activities. This is the first report on the biochemical characterization of a GH46 chitosanase from *C. violaceum*. The biochemical features of *Cv*Csn46 revealed that this enzyme is a useful biocatalyst that can be employed as a molecular tool to produce well-defined, low molecular mass chitosan oligomers, which are promising molecules that can lead to new antifungal products to protect important crops.

Conflict of interest

The authors declare that they have no conflict of interest.

Acknowledgements

This work was supported by research grants from Conselho Nacional de Desenvolvimento Científico e Tecnológico (CNPq) and Coordenação de Aperfeiçoamento de Pessoal de Nível Superior (CAPES). MIGA was recipient of a Master's Fellowship from CNPq.

References

[1] G. Crini, Historical review on chitin and chitosan biopolymers, Environ. Chem. Lett. 17 (2019) 1623–1643. https://doi.org/10.1007/s10311-019-00901-0.

[2] N.A.R. Gow, J.-P. Latge, C.A. Munro, The fungal cell wall: structure, biosynthesis, and function, Microbiol. Spectr. 5 (2017). https://doi.org/10.1128/microbiolspec.FUNK-0035-2016.

[3] R.A.A. Muzzarelli, Chitin Nanostructures in Living Organisms, in: N.S. Gupta (Ed.), Chitin: Formation and Diagenesis, Springer, New York, 2011, pp. 1–34.

[4] S. Beier, S. Bertilsson, Bacterial chitin degradation-mechanisms and ecophysiological strategies, Front. Microbiol. 4 (2013) 149. https://doi.org/10.3389/fmicb.2013.00149.

[5] J.C. Roy, F. Salaün, S. Giraud, A. Ferri, G. Chen, J. Guan, Solubility of Chitin: Solvents, Solution Behaviors and Their Related Mechanisms, in: Z. Xu (Ed.), Solubility of Polysaccharides, InTech, Vienna, Austria, 2017, pp. 109–127. http://dx.doi.org/10.5772/intechopen.71385.

[6] Y. Araki, E. Ito, A pathway of chitosan formation in *Mucor rouxii*: enzymatic deacetylation of chitin, Biochem. Biophys. Res. Commun. 56 (1974) 669–675. https://doi.org/10.1016/0006-291x(74)90657-3.

[7] C.K.S. Pillai, W. Paul, C.P. Sharma, Chitin and chitosan polymers: Chemistry, solubility and fiber formation, Prog. Polym. Sci. 34 (2009) 641–678. https://doi.org/10.1016/j.progpolymsci.2009.04.001.

[8] C. Schmitz, L.G. Auza, D. Koberidze, S. Rasche, R. Fischer, L. Bortesi, Conversion of Chitin to Defined Chitosan Oligomers: Current Status and Future Prospects, Mar. Drugs 17 (2019) 452. https://doi.org/10.3390/md17080452.

[9] R.L. Monaghan, D.E. Eveleigh, R.P. Tewari, E.T. Reese, Chitosanase, a novel enzyme, Nat. New Biol. 245 (1973) 78–80. https://doi.org/10.1038/newbio245078a0.

[10] V. Lombard, H. Golaconda Ramulu, E. Drula, P.M. Coutinho, B. Henrissat, The carbohydrate-active enzymes database (CAZy) in 2013, Nucleic Acids Res. 42 (2014) D490–D495. https://doi.org/10.1093/nar/gkt1178.

[11] P. Viens, M.-È. Lacombe-Harvey, R. Brzezinski, Chitosanases from Family 46 of Glycoside Hydrolases: From Proteins to Phenotypes, Mar. Drugs 13 (2015) 6566–6587. https://doi.org/10.3390/md13116566.

[12] T. Weikert, A. Niehues, S. Cord-Landwehr, M.J. Hellmann, B.M. Moerschbacher, Reassessment of chitosanase substrate specificities and classification, Nat. Commun. 8 (2017) 1698. https://doi.org/10.1038/s41467-017-01667-1.

[13] T. Fukamizo, Y. Honda, S. Goto, I. Boucher, R. Brzezinski, Reaction mechanism of chitosanase from *Streptomyces* sp. N174, Biochem. J. 311 (1995) 377–383. https://doi.org/10.1042/bj3110377.

[14] A. Wohlkönig, J. Huet, Y. Looze, F. Wintjens, Structural relationships in the lysozyme superfamily: significant evidence for glycoside hydrolase signature motifs, PLoS One 5 (2010) e15388. https://doi.org/10.1371/journal.pone.0015388.

[15] I. Boucher, T. Fukamizo, Y. Honda, G.E. Willick, W.A. Neugebauer, R. Brzezinski, Site-directed mutagenesis of evolutionary conserved carboxylic amino acids in the chitosanase from *Streptomyces* sp. N174 reveals two residues essential for catalysis, J. Biol. Chem. 270 (1995) 31077–31082. https://doi.org/10.1074/jbc.270.52.31077.

[16] E.M. Marcotte, A.F. Monzingo, S.R. Ernst, R. Brzezinski, J.D. Robertus, X-ray structure of an anti-fungal chitosanase from *Streptomyces* N174, Nat. Struct. Biol. 3 (1996) 155–162. https://doi.org/10.1038/nsb0296-155.

[17] Y. Kouzai, S. Mochizuki, A. Saito, A. Ando, E. Minami, Y. Nishizawa, Expression of a bacterial chitosanase in rice plants improves disease resistance to the rice blast fungus

Magnaporthe oryzae, Plant Cell Rep. 31 (2012) 629–636. https://doi.org/10.1007/s00299-011-1179-7.

[18] J.A. Koburger, S.O. May, Isolation of *Chromobacterium* spp. from foods, soil, and water, Appl. Environ. Microbiol. 44 (1982) 1463–1465.

[19] A.C.G. Cauz, G.P.B. Carretero, G.K.V. Saraiva, P. Park, L. Mortara, I.M. Cuccovia, M. Brocchi, F.J. Gueiros-Filho, Violacein Targets the Cytoplasmic Membrane of Bacteria, ACS Infect. Dis. 5 (2019) 539–549. https://doi.org/10.1021/acsinfecdis.8b00245.

[20] A. Ciprandi, W.M. da Silva, A.V. Santos, A.M. de Castro Pimenta, M.S.P. Carepo, M.P.C. Schneider, V. Azevedo, A. Silva, *Chromobacterium violaceum*: important insights for virulence and biotechnological potential by exoproteomic studies, Curr. Microbiol. 67 (2013) 100–106. https://doi.org/10.1007/s00284-013-0334-5.

[21] A. Castellani, Viability of some pathogenic fungi in distilled water, J. Trop. Med. Hyg. 42 (1939) 225–226.

[22] B. Webb, A. Sali, Comparative Protein Structure Modeling Using MODELLER, Curr. Protoc. Bioinformatics 47 (2014) 5.6.1-5.6.32. https://doi.org/10.1002/0471250953.bi0506s47.

[23] L. Zimmermann, A. Stephens, S.-Z. Nam, D. Rau, J. Kübler, M. Lozajic, F. Gabler, J. Söding, A.N. Lupas, V. Alva, A Completely Reimplemented MPI Bioinformatics Toolkit with a New HHpred Server at its Core, J. Mol. Biol. 430 (2018) 2237–2243. https://doi.org/10.1016/j.jmb.2017.12.007.

[24] P.H. Malecki, C.E. Vorgias, M.V. Petoukhov, D.I. Svergun, W. Rypniewski, Crystal structures of substrate-bound chitinase from the psychrophilic bacterium *Moritella marina* and its structure in solution, Acta Crystallogr. D Biol. Crystallogr. 70 (2014) 676–684. https://doi.org/10.1107/S1399004713032264.

[25] J. Saito, A. Kita, Y. Higuchi, Y. Nagata, A. Ando, K. Miki, Crystal structure of chitosanase from *Bacillus circulans* MH-K1 at 1.6-Å resolution and its substrate recognition mechanism, J. Biol. Chem. 274 (1999) 30818–30825. https://doi.org/10.1074/jbc.274.43.30818.

[26] M. Berjanskii, Y. Liang, J. Zhou, P. Tang, P. Stothard, Y. Zhou, J. Cruz, C. MacDonell, G. Lin, P. Lu, D.S. Wishart, PROSESS: a protein structure evaluation suite and server, Nucleic Acids Res. 38 (2010) W633–W640. https://doi.org/10.1093/nar/gkq375.

[27] G.M. Morris, R. Huey, W. Lindstrom, M.F. Sanner, R.K. Belew, D.S. Goodsell, A.J. Olson, AutoDock4 and AutoDockTools4: automated docking with selective receptor flexibility, J. Comput. Chem. 30 (2009) 2785–2791. https://doi.org/10.1002/jcc.21256.

[28] O. Trott, A.J. Olson, AutoDock Vina: improving the speed and accuracy of docking with a new scoring function, efficient optimization and multithreading, J. Comput. Chem. 31 (2010) 455–461. https://doi.org/10.1002/jcc.21334.

[29] P.A.C. Maranhão, C.S. Teixeira, D.L. Sousa, I.L. Barroso-Neto, J.E. Monteiro-Júnior, A.V. Fernandes, M.V. Ramos, I.M. Vasconcelos, J.F.C. Gonçalves, B.A.M. Rocha, V.N. Freire, T.B. Grangeiro, cDNA cloning, molecular modeling and docking calculations of L-type lectins from *Swartzia simplex* var. *grandiflora* (Leguminosae, Papilionoideae), a member of the tribe Swartzieae, Phytochemistry 139 (2017) 60–71. https://doi.org/10.1016/j.phytochem.2017.04.007.

[30] F. Ronquist, M. Teslenko, P. van der Mark, D.L. Ayres, A. Darling, S. Höhna, B. Larget, L. Liu, M.A. Suchard, J.P. Huelsenbeck, MrBayes 3.2: efficient Bayesian phylogenetic inference and model choice across a large model space, Syst. Biol. 61 (2012) 539–542. https://doi.org/10.1093/sysbio/sys029.

[31] D. Darriba, D. Posada, A.M. Kozlov, A. Stamatakis, B. Morel, T. Flouri, ModelTest-NG: A New and Scalable Tool for the Selection of DNA and Protein Evolutionary Models, Mol. Biol. Evol. 37 (2020) 291–294. https://doi.org/10.1093/molbev/msz189.

[32] M.A. Miller, T. Schwartz, B.E. Pickett, S. He, E.B. Klem, R.H. Scheuermann, M. Passarotti, S. Kaufman, M.A. O'Leary, A RESTful API for Access to Phylogenetic Tools via the CIPRES Science Gateway, Evol. Bioinform. Online 11 (2015) 43–48. https://doi.org/10.4137/EBO.S21501.

[33] I. Letunic, P. Bork, Interactive Tree Of Life (iTOL) v4: recent updates and new developments, Nucleic Acids Res. 47 (2019) W256–W259. https://doi.org/10.1093/nar/gkz239.

[34] J. Sambrook, E. Fritsch, T. Maniatis, Molecular Cloning: A Laboratory Manual, 2nd ed., Cold Spring Harbor Laboratory Press, Cold Spring Harbor, 1989.

[35] M.D. Lobo, F.D. Silva, P.G. Landim, P.R. da Cruz, T.L. de Brito, S.C. de Medeiros, J.T. Oliveira, I.M. Vasconcelos, H.D. Pereira, T.B. Grangeiro, Expression and efficient secretion of a functional chitinase from *Chromobacterium violaceum* in *Escherichia coli*, BMC Biotechnol. 13 (2013) 46. https://doi.org/10.1186/1472-6750-13-46.

[36] Y.J. Choi, E.J. Kim, Z. Piao, Y.C. Yun, Y.C. Shin, Purification and characterization of chitosanase from *Bacillus* sp. strain KCTC 0377BP and its application for the production of chitosan oligosaccharides, Appl. Environ. Microbiol. 70 (2004) 4522–4531. https://doi.org/10.1128/AEM.70.8.4522-4531.2004.

[37] G.L. Miller, Use of Dinitrosalicylic Acid Reagent for Determination of Reducing Sugar, Anal. Chem. 31 (1959) 426–428. https://doi.org/10.1021/ac60147a030.

[38] R.M. Teather, P.J. Wood, Use of Congo red-polysaccharide interactions in enumeration and characterization of cellulolytic bacteria from the bovine rumen, Appl. Environ. Microbiol. 43 (1982) 777–780.

[39] M.M. Bradford, A rapid and sensitive method for the quantitation of microgram quantities of protein utilizing the principle of protein-dye binding, Anal. Biochem. 72 (1976) 248–254.

[40] U.K. Laemmli, Cleavage of structural proteins during the assembly of the head of bacteriophage T4, Nature 227 (1970) 680–685.

[41] G. Candiano, M. Bruschi, L. Musante, L. Santucci, G.M. Ghiggeri, B. Carnemolla, P. Orecchia, L. Zardi, P.G. Righetti, Blue silver: a very sensitive colloidal Coomassie G-250 staining for proteome analysis, Electrophoresis 25 (2004) 1327–1333. https://doi.org/10.1002/elps.200305844.

[42] A.J. Rocha, B.L. Sousa, M.S. Girão, I.L. Barroso-Neto, J.E. Monteiro-Júnior, J.T.A. Oliveira, C.S. Nagano, R.F. Carneiro, A.C.O. Monteiro-Moreira, B.A.M. Rocha, V.N. Freire, T.B. Grangeiro, Cloning of cDNA sequences encoding cowpea (*Vigna unguiculata*) vicilins: Computational simulations suggest a binding mode of cowpea vicilins to chitin oligomers, Int. J. Biol. Macromol. 117 (2018) 565–573. https://doi.org/10.1016/j.ijbiomac.2018.05.197.

[43] R.F. Carneiro, R.C.F. Torres, K.P. Chaves, M.A. de Vasconcelos, B.L. de Sousa, A.C.R. Goveia, F.V. Arruda, M.N.C. Matos, H. Matthews-Cascon, V.N. Freire, E.H. Teixeira, C.S. Nagano, A.H. Sampaio, Purification, Biochemical Characterization, and Amino Acid Sequence of a Novel Type of Lectin from *Aplysia dactylomela* Eggs with Antibacterial/Antibiofilm Potential, Mar. Biotechnol. 19 (2017) 49–64. https://doi.org/10.1007/s10126-017-9728-x.

[44] A.E.R. Holanda, B.C. Souza, E.C.D. Carvalho, R.S. Oliveira, F.R. Martins, C.R. Muniz, R.C. Costa, A.A. Soares, How do leaf wetting events affect gas exchange and leaf lifespan of plants from seasonally dry tropical vegetation?, Plant Biol. 21 (2019) 1097–1109. https://doi.org/10.1111/plb.13023.

[45] Y. Itoh, J. Watanabe, H. Fukada, R. Mizuno, Y. Kezuka, T. Nonaka, T. Watanabe, Importance of Trp59 and Trp60 in chitin-binding, hydrolytic, and antifungal activities of *Streptomyces griseus* chitinase C, Appl. Microbiol. Biotechnol. 72 (2006) 1176–1184. https://doi.org/10.1007/s00253-006-0405-7.

[46] Y. Kezuka, M. Ohishi, Y. Itoh, J. Watanabe, M. Mitsutomi, T. Watanabe, T. Nonaka, Structural studies of a two-domain chitinase from *Streptomyces griseus* HUT6037, J. Mol. Biol. 358 (2006) 472–484. https://doi.org/10.1016/j.jmb.2006.02.013.

[47] T. Ikegami, T. Okada, M. Hashimoto, S. Seino, T. Watanabe, M. Shirakawa, Solution structure of the chitin-binding domain of *Bacillus circulans* WL-12 chitinase A1, J. Biol. Chem. 275 (2000) 13654–13661.

[48] T. Fukamizo, Y. Honda, S. Goto, I. Boucher, R. Brzezinski, Reaction mechanism of chitosanase from *Streptomyces* sp. N174, Biochem. J. 311 (1995) 377–383. https://doi.org/10.1042/bj3110377.

[49] S.H. Yoon, S.K. Kim, J.F. Kim, Secretory production of recombinant proteins in *Escherichia coli*, Recent Pat. Biotechnol. 4 (2010) 23–29. https://doi.org/10.2174/187220810790069550.

[50] J.V. Krondiris, D.C. Sideris, Intramolecular disulfide bonding is essential for betanodavirus coat protein conformation, J. Gen. Virol. 83 (2002) 2211–2214. https://doi.org/10.1099/0022-1317-83-9-2211.

[51] G. Holzwarth, P. Doty, The Ultraviolet Circular Dichroism of Polypeptides, J. Am. Chem. Soc. 87 (1965) 218–228. https://doi.org/10.1021/ja01080a015.

[52] T.-W. Liang, W.-T. Chen, Z.-H. Lin, Y.-H. Kuo, A.D. Nguyen, P.-S. Pan, S.-L. Wang, An Amphiprotic Novel Chitosanase from *Bacillus mycoides* and Its Application in the Production of Chitooligomers with Their Antioxidant and Anti-Inflammatory Evaluation, Int. J. Mol. Sci. 17 (2016) 1302. https://doi.org/10.3390/ijms17081302.

[53] C. Wurth, U. Kessler, J. Vogt, G.E. Schulz, G. Folkers, L. Scapozza, The effect of substrate binding on the conformation and structural stability of Herpes simplex virus type 1 thymidine kinase, Protein Sci. 10 (2001) 63–73.

[54] Y.-C. Hsieh, Y.-J. Wu, T.-Y. Chiang, C.-Y. Kuo, K.L. Shrestha, C.-F. Chao, Y.-C. Huang, P. Chuankhayan, W.-G. Wu, Y.-K. Li, C.-J. Chen, Crystal structures of *Bacillus cereus* NCTU2 chitinase complexes with chitooligomers reveal novel substrate binding for catalysis: a chitinase without chitin binding and insertion domains, J. Biol. Chem. 285 (2010) 31603–31615.

[55] I. Ben Abdelmalek-Khedher, M.C. Urdaci, F. Limam, J.M. Schmitter, M.N. Marzouki, P. Bressollier, Purification, characterization, and partial primary sequence of a major-maltotriose-producing alpha-amylase, ScAmy43, from *Sclerotinia sclerotiorum*, J. Microbiol. Biotechnol. 18 (2008) 1555–1563.

[56] G. Liu, S. Wu, W. Jin, C. Sun, Amy63, a novel type of marine bacterial multifunctional enzyme possessing amylase, agarase and carrageenase activities, Sci. Rep. 6 (2016) 18726. https://doi.org/10.1038/srep18726.

[57] M.C. Alliegro, Effects of dithiothreitol on protein activity unrelated to thiol-disulfide exchange: for consideration in the analysis of protein function with Cleland's reagent, Anal. Biochem. 282 (2000) 102–106. https://doi.org/10.1006/abio.2000.4557.

[58] R. Singh, T. Weikert, S. Basa, B.M. Moerschbacher, Structural and biochemical insight into mode of action and subsite specificity of a chitosan degrading enzyme from *Bacillus* spec. MN, Sci. Rep. 9 (2019) 1–13. https://doi.org/10.1038/s41598-018-36213-6.

[59] Q. Lyu, Y. Shi, S. Wang, Y. Yang, B. Han, W. Liu, D.N.M. Jones, W. Liu, Structural and biochemical insights into the degradation mechanism of chitosan by chitosanase OU01, Biochim. Biophys. Acta. 1850 (2015) 1953–1961. https://doi.org/10.1016/j.bbagen.2015.06.011.

[60] N. Guo, J. Sun, W. Wang, L. Gao, J. Liu, Z. Liu, C. Xue, X. Mao, Cloning, expression and characterization of a novel chitosanase from *Streptomyces albolongus* ATCC 27414, Food Chem. 286 (2019) 696–702. https://doi.org/10.1016/j.foodchem.2019.02.056.

[61] A. Zhang, Y. He, G. Wei, J. Zhou, W. Dong, K. Chen, P. Ouyang, Molecular characterization of a novel chitinase CmChi1 from *Chitinolyticbacter meiyuanensis* SYBC-H1 and its use in N-acetyl-d-glucosamine production, Biotechnol. Biofuels 11 (2018) 179. https://doi.org/10.1186/s13068-018-1169-x.

[62] Z. Knezevic-Jugovic, Z. Petronijevic, A. Smelcerovic, Chitin and Chitosan from Microorganisms, in: S. Kim (Ed.), Chitin, Chitosan, Oligosaccharides and Their Derivatives: Biological Activities and Applications, CRC Press, Boca Raton, 2011, pp. 25–36.

[63] T. Fukamizo, Y. Honda, H. Toyoda, S. Ouchi, S. Goto, Chitinous component of the cell wall of *Fusarium oxysporum*, its structure deduced from chitosanase digestion, Biosci. Biotechnol. Biochem. 60 (1996) 1705–1708. https://doi.org/10.1271/bbb.60.1705.

[64] Y. Matsuda, Y. Iida, T. Shinogi, K. Kakutani, T. Nonomura, H. Toyoda, *In Vitro* Suppression of Mycelial Growth of *Fusarium oxysporum* by Extracellular Chitosanase of *Sphingobacterium multivorum* and Cloning of the Chitosanase Gene csnSM1, J. Gen. Plant Pathol. 67 (2001) 318–324. https://doi.org/10.1007/PL00013039.

[65] C.R. Muniz, F.C.O. Freire, F.M.P. Viana, J.E. Cardoso, P. Cooke, D. Wood, M.I.F. Guedes, Colonization of cashew plants by *Lasiodiplodia theobromae*: Microscopical features, Micron 42 (2011) 419–428. https://doi.org/10.1016/j.micron.2010.12.003.

[66] R.C. Summerbell, S. Krajden, R. Levine, M. Fuksa, Subcutaneous phaeohyphomycosis caused by *Lasiodiplodia theobromae* and successfully treated surgically, Med. Mycol. 42 (2004) 543–547. https://doi.org/10.1080/13693780400005916.

[67] S. Saha, J. Sengupta, D. Banerjee, A. Khetan, *Lasiodiplodia theobromae* keratitis: a case report and review of literature, Mycopathologia 174 (2012) 335–339. https://doi.org/10.1007/s11046-012-9546-7.

[68] J. Palma-Guerrero, J.A. Lopez-Jimenez, A.J. Pérez-Berná, I.-C. Huang, H.-B. Jansson, J. Salinas, J. Villalaín, N.D. Read, L.V. Lopez-Llorca, Membrane fluidity determines sensitivity of filamentous fungi to chitosan, Mol. Microbiol. 75 (2010) 1021–1032. https://doi.org/10.1111/j.1365-2958.2009.07039.x.

[69] A. Aranda-Martinez, F. Lopez-Moya, L.V. Lopez-Llorca, Cell wall composition plays a key role on sensitivity of filamentous fungi to chitosan, J. Basic Microbiol. 56 (2016) 1059–1070. https://doi.org/10.1002/jobm.201500775.

[70] A. Saito, T. Ooya, D. Miyatsuchi, H. Fuchigami, K. Terakado, S. Nakayama, T. Watanabe, Y. Nagata, A. Ando, Molecular characterization and antifungal activity of a family 46 chitosanase from *Amycolatopsis* sp. CsO-2, FEMS Microbiol. Lett. 293 (2009) 79–84. https://doi.org/10.1111/j.1574-6968.2009.01507.x.

[71] M. Tomita, A. Kikuchi, M. Kobayashi, M. Yamaguchi, S. Ifuku, S. Yamashoji, A. Ando, A. Saito, Characterization of antifungal activity of the GH-46 subclass III chitosanase from *Bacillus circulans* MH-K1, Antonie Van Leeuwenhoek 104 (2013) 737–748. https://doi.org/10.1007/s10482-013-9982-5.

[72] B. Yuan, P.-Y. Xu, Y.-J. Zhang, P.-P. Wang, H. Yu, J.-H. Jiang, Synthesis of biocontrol macromolecules by derivative of chitosan with surfactin and antifungal evaluation, Int. J. Biol. Macromol. 66 (2014) 7–14. https://doi.org/10.1016/j.ijbiomac.2014.02.011.

[73] K. Xing, Y. Xing, Y. Liu, Y. Zhang, X. Shen, X. Li, X. Miao, Z. Feng, X. Peng, S. Qin, Fungicidal effect of chitosan via inducing membrane disturbance against *Ceratocystis fimbriata*, Carbohydr. Polym. 192 (2018) 95–103. https://doi.org/10.1016/j.carbpol.2018.03.053.

[74] M. Riquelme, J. Aguirre, S. Bartnicki-García, G.H. Braus, M. Feldbrügge, U. Fleig, W. Hansberg, A. Herrera-Estrella, J. Kämper, U. Kück, R.R. Mouriño-Pérez, N. Takeshita, R. Fischer, Fungal Morphogenesis, from the Polarized Growth of Hyphae to Complex Reproduction and Infection Structures, Microbiol. Mol. Biol. Rev. 82 (2018) e00068-17. https://doi.org/10.1128/MMBR.00068-17.

[75] M.A. Matica, F.L. Aachmann, A. Tøndervik, H. Sletta, V. Ostafe, Chitosan as a Wound Dressing Starting Material: Antimicrobial Properties and Mode of Action, Int. J. Mol. Sci. 20 (2019) 5889. https://doi.org/10.3390/ijms20235889.

[76] Y. Sui, Z. Ma, X. Meng, Proteomic analysis of the inhibitory effect of oligochitosan on the fungal pathogen, *Botrytis cinerea*, J. Sci. Food Agric. 99 (2019) 2622–2628. https://doi.org/10.1002/jsfa.9480.

[77] M. Adeolu, R.S. Gupta, Phylogenomics and molecular signatures for the order Neisseriales: proposal for division of the order Neisseriales into the emended family Neisseriaceae and Chromobacteriaceae fam. nov, Antonie Van Leeuwenhoek 104 (2013) 1–24. https://doi.org/10.1007/s10482-013-9920-6.

Figure captions

Fig. 1. Domain architecture of *Cv*Csn46 (A) and the occurrence of structurally related proteins in the genomes of *Chromobacterium* species (B). (A) Graphical representation of *Cv*Csn46 regions and domains. (B) Bayesian majority rule consensus tree of the genus *Chromobacterium*. The phylogenetic analysis was performed using the concatenated alignments of amino acid sequences from 19 housekeeping proteins (argRS, dnaK, EF-G, gyrA, gyrB, ileRS, recA, ribosomal proteins S2, S3, S9, L2, and L5, rpoB, rpoC, secY, thrRS, trpRS1, trpRS2 and uvrD), obtained from *Chromobacterium* proteomes (Table S3). The selection of these proteins was based on the previous work by Adeolu and Gupta [77]. Red branches correspond to taxa that contain proteins structurally related to *Cv*Csn46 from *C. violaceum* ATCC 12472. Numbers next to branch nodes are Bayesian posterior probabilities. Proteins from *Iodobacter fluviatilis* (Chromobacteriaceae) strains were set as outgroups.

Fig. 2. Structural features of the chitin-binding domain of *Cv*Csn46. (A) Alignment of the ChBD of *Cv*Csn46 with related sequences from other proteins: *Streptomyces griseus* chitinase C (*Sg*ChiC; PDB ID: 2D49), *Pseudoalteromonas piscicida* chitinase A (*Pp*ChiA; GenBank accession number: P32823), *Brevibacillus laterosporus* GI-9 chitodextrinase (*Bl*Chidex; GenBank accession number: CCF12514), *Vibrio furnissii* chitodextrinase EndoI (*Vf*Chidex; GenBank accession number: P96156), *Bacillus cellulosilyticus* DSM 2522 endoglucanase A (BcEngA; GenBank accession number: P06566) and *Pseudoalteromonas piratica* S8 family serine peptidase (*Pp*SerPep; GenBank accession number: WP_040136598). Sites containing residues that are involved in the interaction of the ChBD of *Sg*ChiC with chitin are indicated by hash marks (B) Cartoon representation of a three-dimensional molecular model of the ChBD of *Cv*Csn46 (green β-strands). The generated model was validated by stereochemical quality analysis (Table S4 and Fig. S14) and aligned to the three-dimensional structure of the ChBD from *Sg*ChiC (cyan β-strands; PDB ID: 2D49). Percentages of sequence identity and

similarity between the primary structures of the ChBDs of *Cv*Csn46 and *Sg*ChiC are 42.5% and 57.5%, respectively. Side chains of aromatic residues involved in substrate-binding are shown as green (*Cv*Csn46) and cyan (*Sg*ChiC) sticks.

Fig. 3. Alignment of the CatD of *Cv*Csn46 with representative structures of the superfamily chitosanase. The CatD primary structure of *Cv*Csn46 was aligned with GH46 chitosanase structures from *Bacillus circulans* (*Bc*Csn46; PDB ID: 1QGI), *Streptomyces* sp. SirexAA-E (*Strep*Csn46; PDB ID: 4ILY) and *Pseudomonas* sp. LL2 (2010) (*Pseudo*Csn46; PDB ID: 4OLT). Sites of residues involved in catalysis and substrate-binding are indicated by triangles and hash marks, respectively. The disulfide bridge between Cys^{151} and Cys^{225}, as predicted by homology modeling of the three-dimensional structure of the CatD of *Cv*Csn46, is indicated by connecting orange line.

Fig. 4. Three-dimensional molecular model of the CatD of *Cv*Csn46 (A) and binding mode of a chitosan fragment in the substrate-binding cleft (B and C). (A) Cartoon representation of the modeled structure, which was validated by stereochemical quality analysis (Table S5 and Fig. S15). The side chains of the 3 residues involved in catalysis are shown as sticks. (B) Transparent molecular surface representation. A chitooligosaccharide [$(GlcN)_2(GlcNAc)_1$] molecule (yellow) docked in the substrate-binding groove is shown as a stick model (N and O atoms are colored blue and red, respectively). Sugar units occupying the subsites −2, −1 and +1 are indicated. (C) Detailed view of the $(GlcN)_2(GlcNAc)_1$ molecule bound in the catalytic cleft of *Cv*Csn46. Hydrogen bonds are shown as red dotted lines and the side chains of interacting residues are depicted as sticks. Water molecules are represented as gray spheres.

Fig. 5. Electrophoretic profile and enzymatic activity of the purified chitosanase *Cv*Csn46 expressed in *Escherichia coli*. (A) The purified protein (25 µg, lane 1) was treated with 5% β-mercaptoethanol and subjected to SDS-PAGE (15% polyacrylamide), as described in the methods section. Lane M: molecular weight markers. The identity of the protein bands as

*Cv*Csn46 was performed using LC-ESI-MS/MS analysis of tryptic peptides. Representative fragmentation spectra are shown on the right side of the gel image. (B) Degradation of polymeric chitosan by *Cv*Csn46, as revealed by an agar plate assay (1, distilled water; 2, 15 µg secreted proteins of *E. coli* cells expressing *Cv*Csn46; 3, 15 µg purified *Cv*Csn46) (C) Plot of initial reaction velocities *vs* substrate concentration.

Fig. 6. Enzymatic characterization of the recombinant chitosanase *Cv*Csn46. (A) Effect of pH on the hydrolytic activity of *Cv*Csn46 measured at 50 °C for 30 min (black line), and effect of different pH values on the stability of *Cv*Csn46 (red line; residual activity was measured at pH 6.0 and 50 °C for 30 min after incubation of the recombinant product with different buffers for 24 h at 25 °C). (B) Effect of temperature on the catalytic activity of *Cv*Csn46 assayed at pH 6.0 (black line), and thermostability of *Cv*Csn46 (red line; residual activity was determined at pH 6.0 and 50 °C after incubation of the recombinant enzyme at different temperatures for 1 h). (C, D) Effects of cations ions (C) and chemical reagents (D) on the chitosanolytic activity of *Cv*Csn46. Residual activity was determined at pH 6.0 and 50 °C after incubation of *Cv*Csn46 with the different cations and chemical reagents for 1 h at 30 °C. All enzymatic assays (panels A, B, C and D) were performed in triplicate (data are means ± standard deviations), as described in the methods section. In panels C and D, means that are significantly different ($P < 0.05$; Bonferroni's multiple comparisons test) when compared to control are indicated by asterisks.

Fig. 7. ESI-MS analysis (positive ion mode) of enzymatic products released from colloidal chitosan incubated with *Cv*Csn46. Bottom image: mass spectrum of products released from 1% colloidal chitosan incubated with 5 µg/mL *Cv*Csn46 for 24 h at pH 6.0 and 50 °C. Top image: MS/MS spectrum of product at *m*/*z* 502.1. The schematic fragmentation of $(GlcN)_3$ (calculated mass = 501.48 Da), and resulting product ions, are shown next to *m*/*z* 502.1.

Fig. 8. *In vitro* antifungal activity of chitooligosaccharides (COS) obtained from the hydrolytic action of *Cv*Csn46 on polymeric chitosan. Top image: Curves of mycelium growth of *L. theobromae* CCJ-184 cultivated on PDA plates containing water, COS (doses = 0.25, 0.5, 1.0 and 2 mg) or Carbendazim (5 µg). Each point represents the mean ± standard deviation of the diameter of each fungus colony, as shown in Fig. S17. When compared to colonies grown in the presence of water, the mean diameters of colonies that grew in the presence of different doses of COS were significantly lower (*) at time points of 24 h, 48 h, 72 h and 96 h ($P < 0.0001$; Bonferroni's multiple comparisons test). Bottom image: SEM images of untreated mycelium (A-C), mycelium treated with COS (dose = 2 mg) (D-G) and mycelium treated with 5 µg Carbendazim (H-I). The assays to evaluate the morphological alterations in *L. theobromae* CCJ-184 grown *in vitro* in the presence of COS and acquisition of SEM images were performed as described in the Methods section.

International Journal of Biological Macromolecules
Azevedo et al.
Figure 1

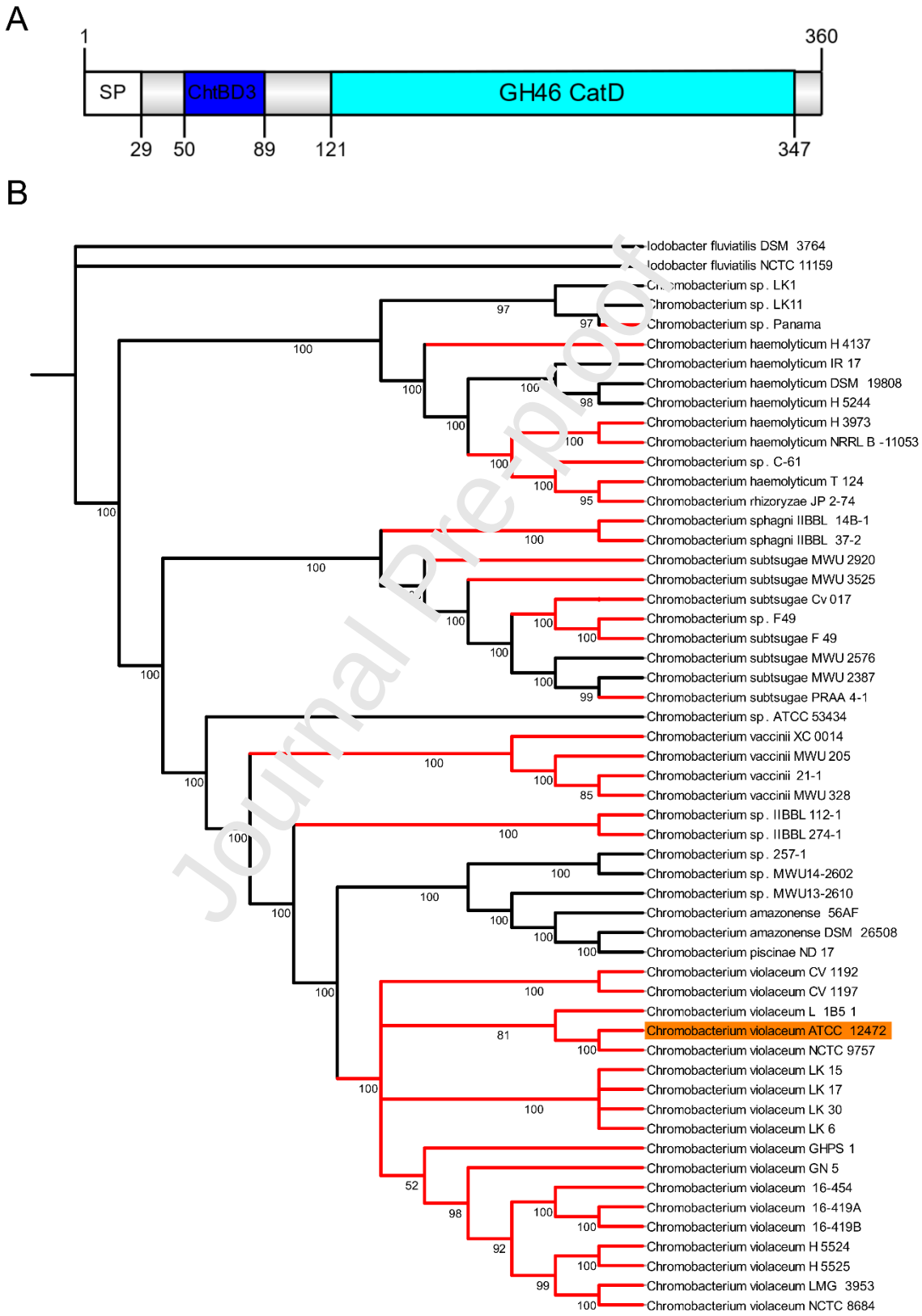

International Journal of Biological Macromolecules
Azevedo et al.
Figure 2

A

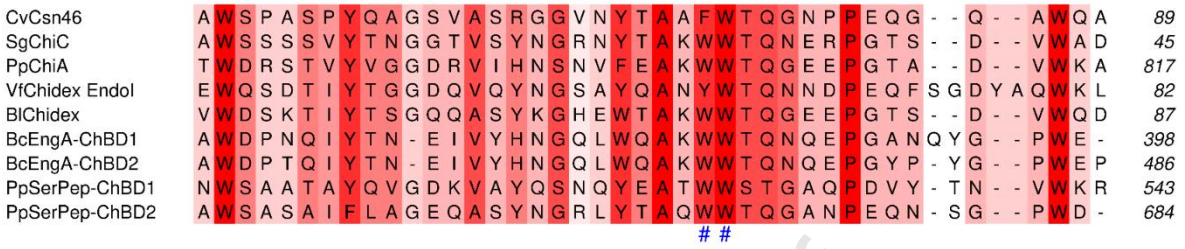

B

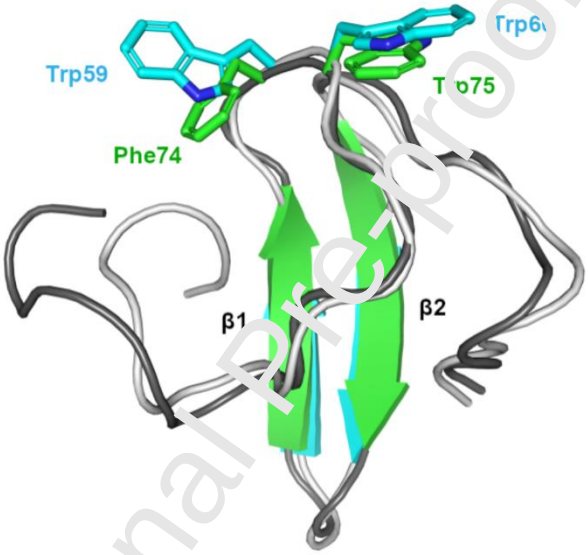

International Journal of Biological Macromolecules
Azevedo et al.
Figure 3

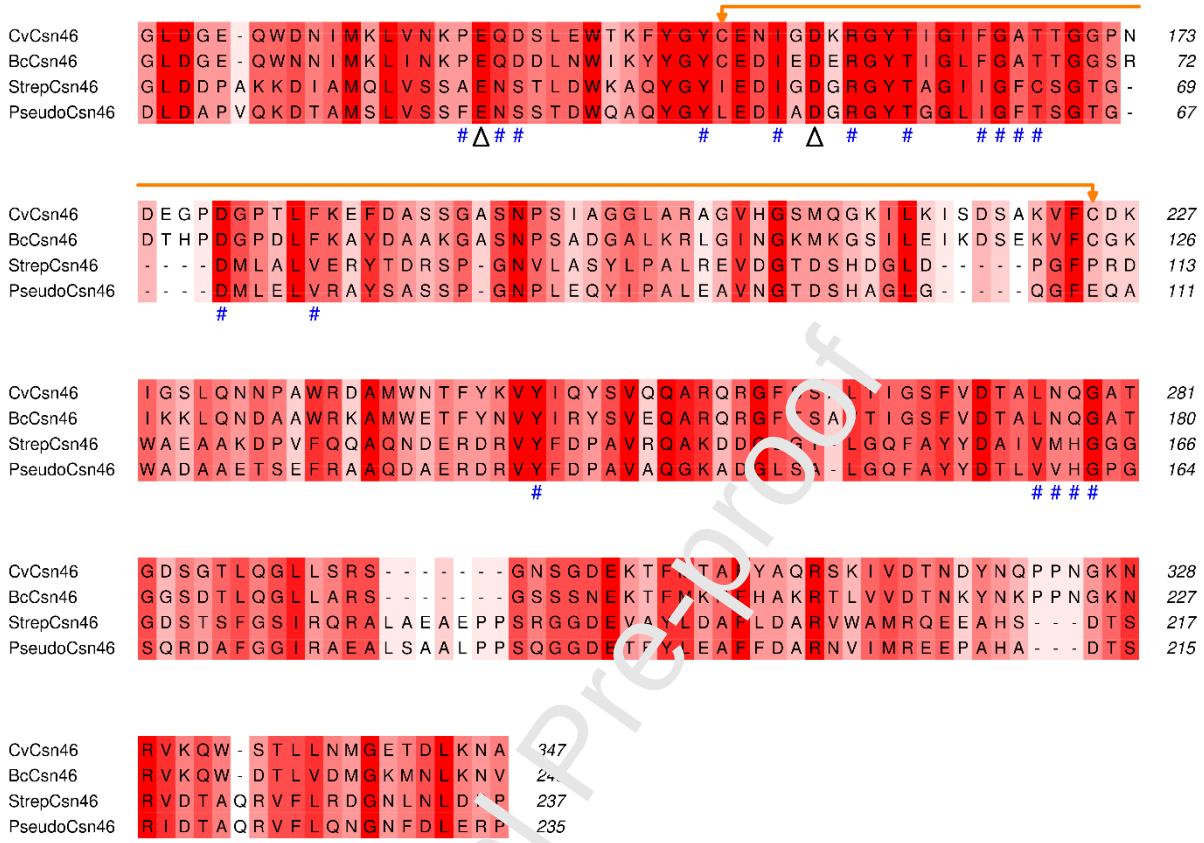

International Journal of Biological Macromolecules
Azevedo et al.
Figure 4

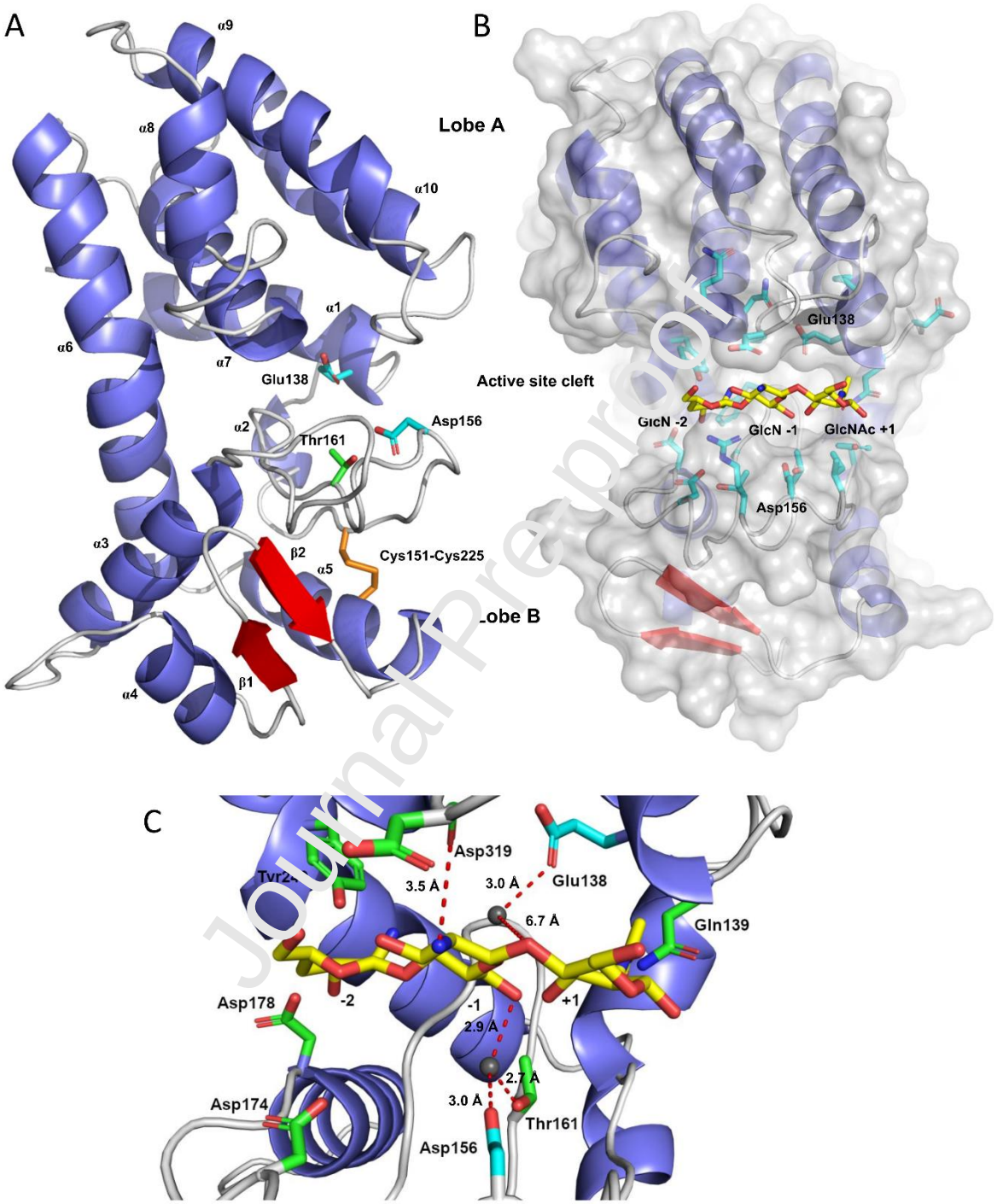

International Journal of Biological Macromolecules
Azevedo et al.
Figure 5

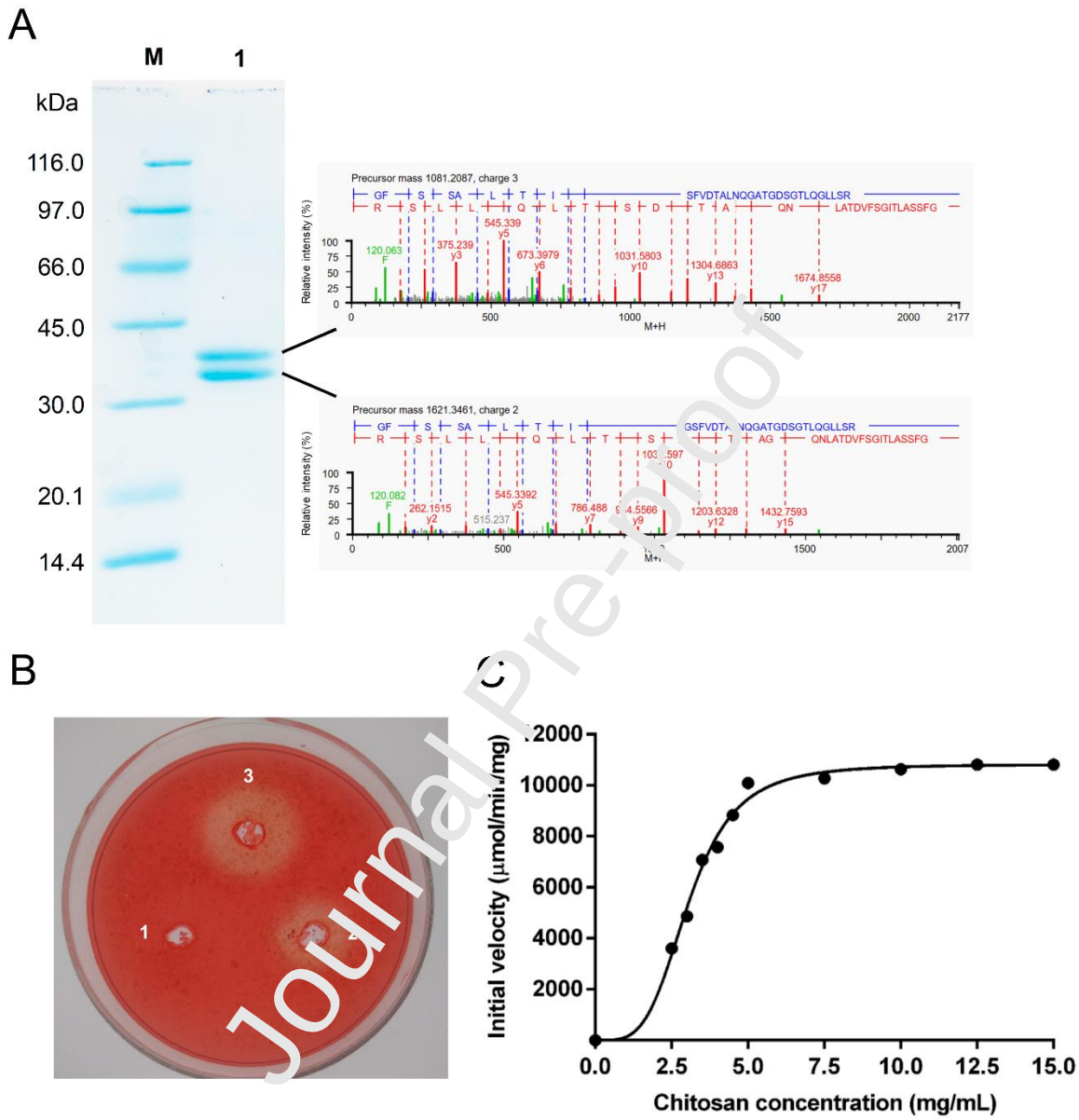

International Journal of Biological Macromolecules
Azevedo et al.
Figure 6

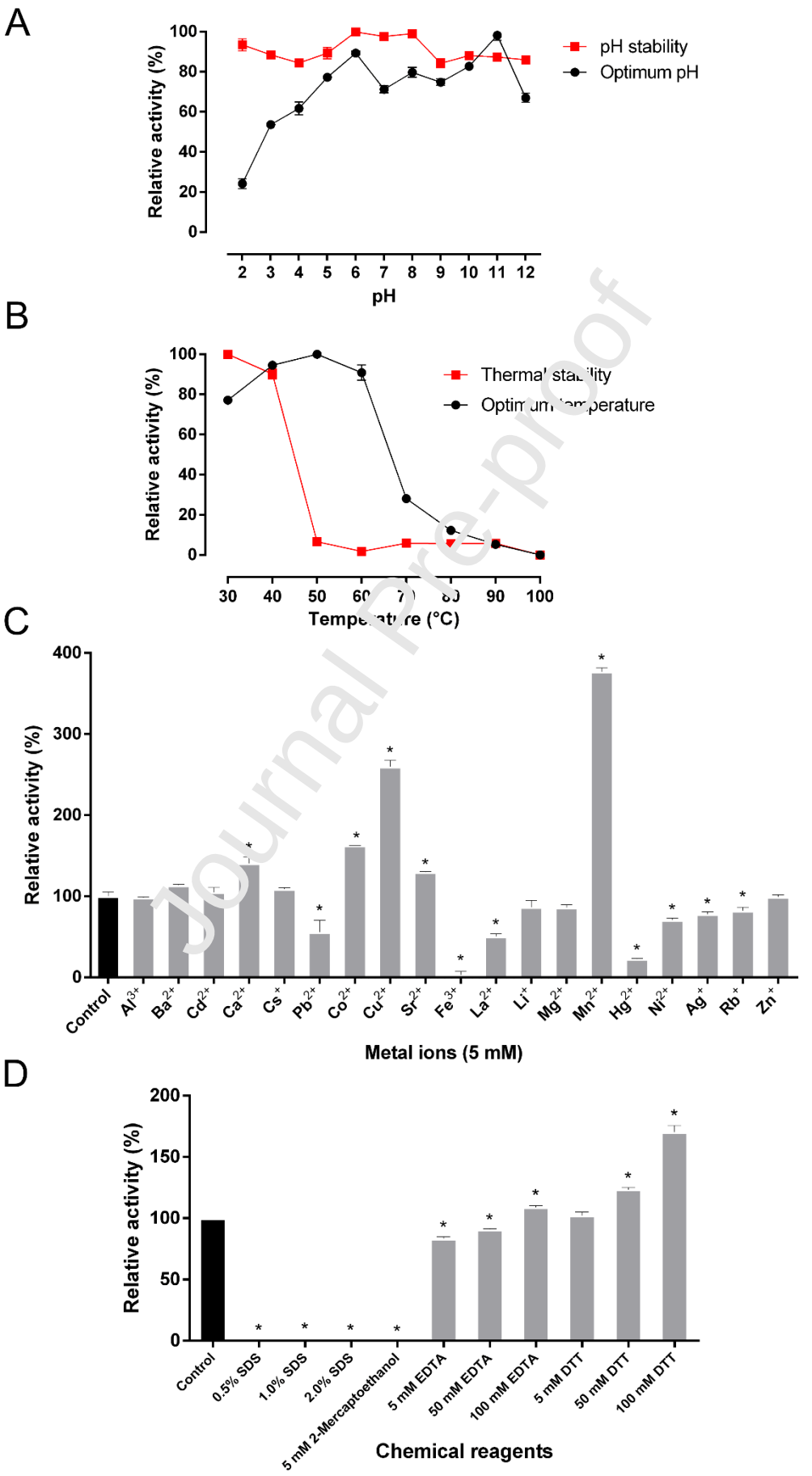

International Journal of Biological Macromolecules
Azevedo et al.
Figure 7

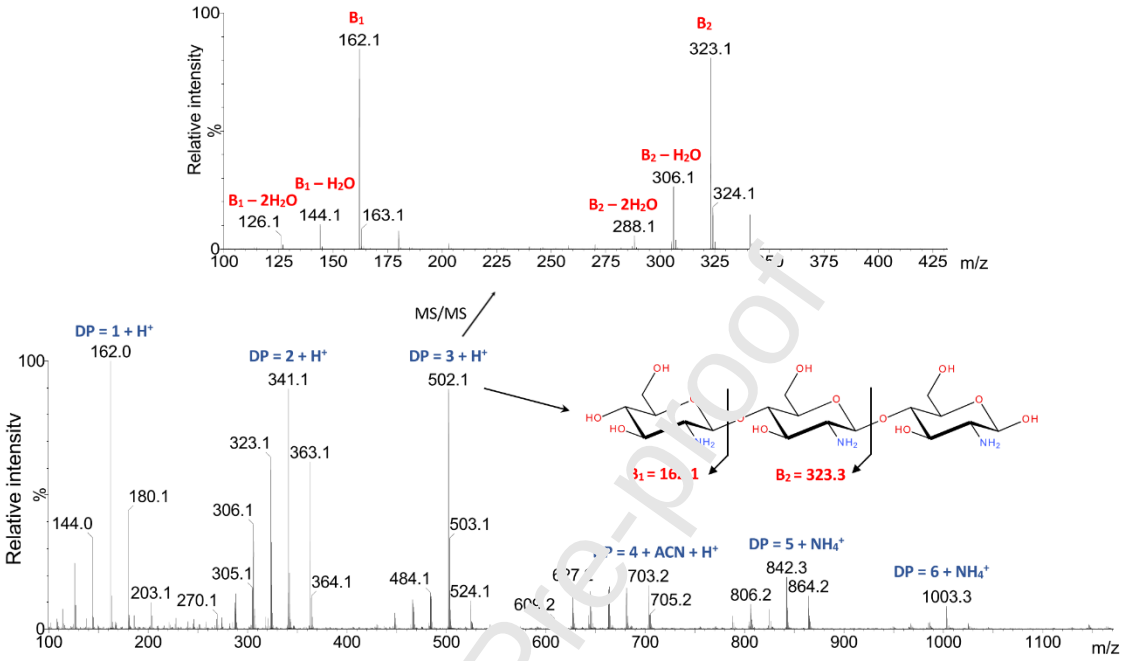

International Journal of Biological Macromolecules
Azevedo et al.
Figure 8

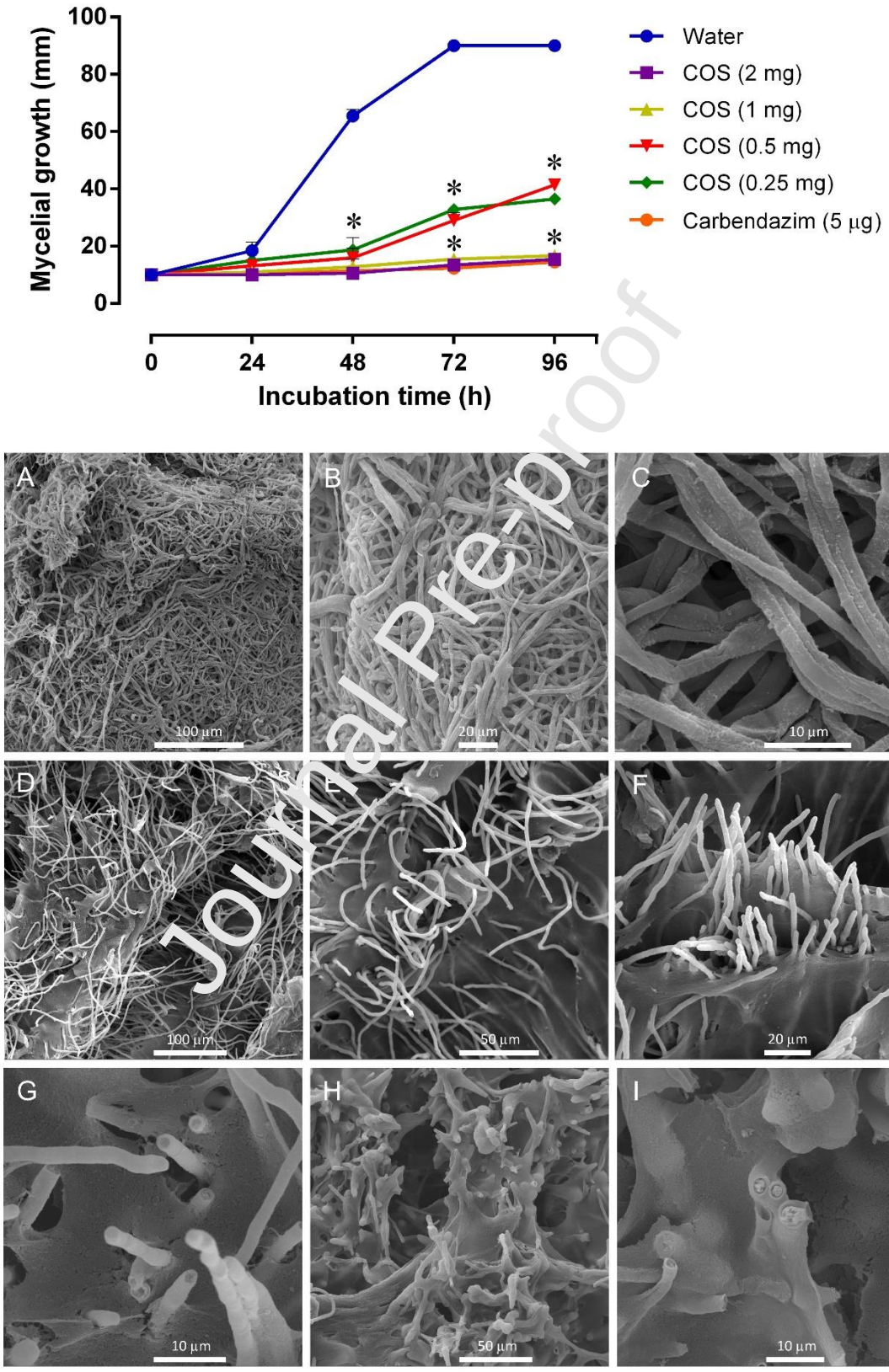

Author statement

The authors declare that the manuscript entitled “Secretory production in *Escherichia coli* of a GH46 chitosanase from *Chromobacterium violaceum*, suitable to generate antifungal chitooligosaccharides”, has not been published previously and that it is not under consideration for publication elsewhere. Authors also declare that they do not have any potential conflicts of interest.

Highlights

- A GH46 chitosanase from *Chromobacterium violaceum* was produced in *Escherichia coli*.
- The recombinant protein (*Cv*Csn46) was purified and partially characterized.
- *Cv*Csn46 had an amphiprotic behavior, with highest activity at pH values 6.0 and 11.0.
- The enzyme degraded chitosan through dual, endo- and exo-type hydrolytic activities.
- Low molecular mass chitosan oligomers produced by *Cv*Csn46 showed antifungal activity.